# Soil weathering and accumulation rates of oxalate-extractable phases derived from alpine chronosequences of up to 1Ma in age

Dahms, Dennis ; Favilli, Filippo ; Krebs, Rolf ; Egli, Markus

Abstract: In this study we compare newly-developed chemical weathering data with previously published data from soils developed along two chronosequences of glacial deposits in the European Alps and the Rocky Mountains (Wind River Range, USA). By combining these chronosequences, we are able to present a comprehensive dataset that represents a time period of >1 Ma. We describe weathering trends of important elements using a number of weathering indices (e.g., K + Ca/Ti ratio, the weathering 'index B' of Kronberg and Nesbitt (1981) and the open mass transport function). Further, we describe the accumulation of Al, Fe, Si and Mn oxyhydroxides (including partially organic phases) as a function of time, and derive the corresponding accumulation rates. We calculated pedogenetically formed oxyhydroxides using an approach based on immobile elements. Our study represents one of only a few studies that describe rates of soil chemical weathering over a period as long as 1 Ma. Results show that rates of chemical weathering clearly decrease along the chronosequences with increasing age of the soils. We find weathering rates are nearly four orders of magnitude lower in the 1 Ma-old soils than in the young soils. Our results suggest that the older soils may be reaching a steady state for these chemical properties in their present environments. A power function best explains the measured time-trends of the 'index B' and (K+Ca)/Ti) ratios in the soils. The best time-trend model for pedogenic weakly- to poorly crystalline phases and the relative losses/gains (based on the open-system mass transport function) were obtained with an exponential decay model function. In terms of the soil system, the decreases in the accumulation rate of the oxyhydroxides appears to be influenced not only by the factor of time but by climate as well (increased precipitation at higher altitudes slows the decrease in weathering rate over time). Thus, our 1 Ma chronosequences also become pedogenic gradients since we describe variations in soil properties along biogenic gradients.

DOI: https://doi.org/10.1016/j.geomorph.2012.01.021

# Soil weathering and accumulation rates of oxalate-extractable phases derived from alpine chronosequences of up to 1 Ma in age

Dennis Dahms[1], Filippo Favilli[2], Rolf Krebs[3], Markus Egli[4]*

[1]Department of Geography, University of Northern Iowa, Cedar Falls, USA

[2]Institute of Biometeorology, CNR, Florence, Italy

[3]Institute of Natural Resource Sciences, Zurich University of Applied Sciences, Wädenswil, Switzerland

[4]Department of Geography, University of Zurich, CH-8057 Zurich, Switzerland

*E-mail of the corresponding author: markus.egli@geo.uzh.ch

## Abstract

In this study we compare newly-developed chemical weathering data with previously published data from soils developed along two chronosequences of glacial deposits in the European Alps and the Rocky Mountains (Wind River Range, USA). By combining these chronosequences, we are able to present a comprehensive dataset that represents a time period of ≥1 Ma. We describe weathering trends of important elements using a number of weathering indices (e.g, K+Ca/Ti ratio, the weathering 'index B' of Kronberg and Nesbitt (1981) and the open mass transport function). Further, we describe the accumulation of Al, Fe, Si and Mn oxyhydoxides (including partially organic phases) as a function of time, and derive the corresponding accumulation rates. We calculated pedogenetically formed oxyhydroxides using an approach based on immobile elements. Our study represents one of only a few studies that describe rates of soil chemical weathering over a period as

long as ~1 Ma. Results show that rates of chemical weathering clearly decrease along the chronosequences with increasing age of the soils. We find weathering rates are nearly four orders of magnitude lower in the 1 Ma-old soils than in the young soils. Our results suggest that the older soils may be reaching a steady state for these chemical properties in their present environments. A power function best explains the measured time-trends of the 'index B' and (K+Ca)/Ti) ratios in the soils. The best time-trend model for pedogenic weakly- to poorly crystalline phases and the relative losses/gains (based on the open-system mass transport function) was obtained with an exponential decay model function. In terms of the soil system, the decreases in the accumulation rate of the oxyhydroxides appears to be influenced not only by the factor of time but by climate as well (increased precipitation at higher altitudes slows the decrease in weathering rate over time). Thus, our ~1 Ma chronosequences also become pedogenic gradients since we describe variations in soil properties along biogenic gradients.

Keywords: Chronosequence, pedogenic gradient, soils, weathering, steady state, Alps, Wind River Range

## 1. Introduction

Weathering rates or rates of element depletion or accumulation on the catchment or profile scale are often obtained by mass balance studies (input-output budgets) and give important indications about the reactivity of a corresponding soil or catchment (e.g. April et al, 1986; Johnson and Lindberg, 1992; Wright et al., 1992; Bain et al., 1994; Drever, 1997; Olsson and Melkerud, 2000; Bernasconi et al., 2011 etc.). Three techniques have commonly been applied to measure rates of chemical weathering (Porder et al., 2007): a) quantification of mass loss from minimally eroded soils of known age using chronosequences (Jenny, 1941; Taylor and Blum, 1995), b) catchment-scale river sampling (e.g. White and Blum, 1995; Riebe et al., 2004), and laboratory experiments (e.g. White and

Brantley, 2003). All three approaches are subject to some uncertainties.

The time over which natural chemical weathering occurs (White and Hochella, 1992) can usually not be reproduced by experimental studies (see White and Brantley, 2003). Chronosequences are useful for estimating field weathering rates (element depletion rates, mineral transformation rates etc.; e.g. Föllmi et al., 2009a,b; Mavris et al., 2011 etc.) and also permit the differentiation of surfaces of differing age (e.g. Fitze, 1982; Dahms, 2002, 2004).

Soil development, in the chemical sense, can be considered as roughly synonymous with weathering (Bohn et al., 1985). Thus, studying characteristics of soil weathering over time may give insight into the influence of time on the rates of chemical weathering. According to Jenny (1941), soils are understood to develop under the influence of the following state factors: parent material, climate, topography, biological activity and time. In order to be quantitatively useful, Jenny (1941) suggested treating the state factors as independent variables, in the sense that field locales exist where the factors can be considered to vary independently. The ways in which a factor is considered to be independent are: (1) if the range of variability of the factor is quite small, and (2) if variation in the factor is large, it has only a negligible effect on the property studied. Thus, a sequence of soils formed on progressively older landscapes is considered a chronosequence, and the quantitative variability of a characteristic along these landscapes is a chronofunction (Birkeland, 1999; Mahaney et al., 2011).

Pedogenic gradients are defined as the variations in soil properties along bioclimatic gradients (Tedrow 1968, 1977; Birkeland et al., 1989) and often are determined by analysing soil chronosequences (Bockheim, 1980; Jenny 1980; Birkeland 1984; Birkeland et al., 1989). Soil chronosequences can provide information about the weathering regimes, soil morphogenesis (see Mahaney et al., 2011) and have greatly advanced our understanding of short- to long-term landscape processes (Milner et al., 2007; Walker et al., 2010). Soil development has been successfully correlated to land surface age in several regions, although in some case such studies were complicated by ero-

76 sion and sedimentation as well as possible tectonic activity (Scarciglia et al., 2006; Sauer et al.,
77 2010). Thus, the study of chronosequences has a long tradition, and both ecologists and soil scien-
78 tists have used the concept of substituting space for time to understand ecosystem and soil evolution
79 (see Ruhe and Walker, 1968; Gile et al., 1981; Walker and del Moral, 2003; Walker et al., 2010;
80 Bernasconi et al., 2011).
81 Soils sampled on moraines and other glacial and periglacial deposits such as rock glaciers can either
82 be helpful indicators to estimate the (relative) age of the landform or, provided that independent
83 dating is available, to derive rates of different time-dependent processes (Egli et al., 2001, 2003;
84 Munroe, 2008; Schaller et al., 2009). Weathering indexes or clay mineral assemblages may provide
85 a differentiation of soils even within a relatively narrow time range and give insight into processes
86 that have occurred at the specific sites. When used as an age indicator, soil development data, how-
87 ever, should be combined with other relative or numerical age data (Birkeland, 1973; Dahms, 2004;
88 Böhlert et al., 2011a) because soil development is, in many respects, not a linear process and
89 chronosequences may be perturbed by the other state factors.
90 Chemical and mineralogical analyses of soil chronosequences offer several methods of distinguish-
91 ing landforms of different ages based on their weathering state (Alexander and Burt, 1996; Evans,
92 1999; Egli et al., 2001, 2003). Well-known soil age indicators are for instance soil pH, rubification,
93 transformation of pedogenic Fe and Al (Birkeland, 1999) and the presence of clay minerals such as
94 smectite (Righi et al., 1999). However, several of them are not applicable to soils in alpine areas as
95 the greatest changes in soil properties occur within approximately 3000 – 4000 years, asymptoti-
96 cally reaching a kind of limiting value after about 15 ky (cf. Fitze, 1982; Egli et al., 2001) and no
97 real changes are observable thereafter.
98 The effects of time on weathering rates can be seen in systematic decreases in natural rates in pro-
99 gressively older weathering environments (e.g. Egli et al, 2001; White and Brantley, 2003). Over
100 centuries to millennia, the rates of primary mineral depletion and secondary clay and metal oxide

formation progressively decrease with soil (surface) age (Taylor and Blum, 1995; Hodson et al., 1999; Stewart et al., 2001, Egli et al., 2001).

Chronosequences often have only a very limited number of data points (and sites) because the plot of only 1 single point (e.g. elemental leaching rates over a whole soil profile) requires intensive laboratory analyses. Here we compare the trends with time of published weathering data obtained from the European Alps with newly-developed data from the Rocky Mountains (Wind River Range, USA; Fig. 1). This technique enables us to present a set of comprehensive data over a time range of c. 1 Ma. This also allows us to reduce the influence of spatial variability on weathering trends for a robust view of soil weathering over an extended timescale.

Datasets reporting the weathering rates of elements over millennia up to 1 Ma are, furthermore, rare. As weathering occurs, secondary mineral phases form that initially have poorly or weakly crystalline characteristics. Only few datasets exist for long-term trends in production or accumulation rates of oxyhydroxides (Fe, Al) (e.g. Birkeland et al., 1989).

## 2. Study sites

We compared new and previously-published datasets on soil chronosequences in order to differentiate trends within several alpine regions and to complete trends with additional data. The sites from Stough Creek Basin in the Wind River Range (WRR) are comparable with sites from the European Alps; soils from Sinks Canyon (WRR), however, have no Alpine correlates in this study. All Alpine and WRR soils developed in glacial deposits whose ages have been previously correlated to known glacial stages of the Rocky Mountains and the European Alps. Parent material is granitic glacial till at all the Wyoming sites, while soils at the Alpine sites were mostly developed in till (different types of moraines) but in some cases relict rock glaciers.

126 The mean annual precipitation and temperature of the individual investigation sites are given in Ta-
127 bles 1 and 2. In general, the European sites have a moister climate (1100 – 2000 mm/y) than the
128 Wind River Range (up to 1000 mm/yr in Stough Creek Basin, but only 340 mm/yr in Sinks Can-
129 yon). Depending on the age and climatic zone of the deposits, pioneer plant communities, shrubs or
130 grassland and forest vegetation is present.
131 Pedogenesis through the observed time frame has not been continuous and completely similar. Cli-
132 mate variability over the past ~1 Ma has been considerable. During the Holocene and Late Pleisto-
133 cene (last 20 ky), however, the climatic variability at the Wind River Range and Alpine sites can be
134 considered as more or less similar (see also Böhlert at al., 2011a). Because of the extreme age of
135 some of the soils in the Wind River Range (>500 ka) some sites have experienced several warm and
136 cold phases. These soils consequently integrate the effect of such climatic variations. For example,
137 soils developed on Bull Lake-age piedmont moraines (~130 ka, OIS-6) of the WRR show thinner,
138 coarser A-horizons than those on adjacent soils developed in Pinedale-age moraines (LGM, OIS-2).
139 This anomaly was created when Foehn winds off the active Pinedale glaciers stripped the finer par-
140 ticles out of the Bull Lake soils. This process also caused A-horizon processes to affect the upper B-
141 horizons of these soils (Hall, 1999; Applegarth and Dahms, 2001). We assume similar processes
142 also were active on older deposits/soils.
143 Age control of the sites is provided by geomorphologic mapping and relative age-relationships
144 (Maisch, 1981, 1992; Dahms, 2002, 2004), surface exposure dating ($^{10}$Be, $^{26}$Al) and radiocarbon
145 dating (Tables 1 and 2; for the WRR: Dahms, 2004; Fabel et al., 2004; and for the Alps: Hantke,
146 1983; Keller and Krayss, 1993; Wipf, 2001; Keller and Krayss, 2005; Maisch et al., 2005; Ivy-Ochs
147 et al., 2007; Favilli et al., 2009; Egli et al., 2010; Böhlert et al., 2011b).
148 The moraines in the Alps could usually be clearly attributed to glacial stages: e.g. Late Glacial
149 Maximum (or soon thereafter), Daun (Oldest Dryas), Egesen (Younger Dryas; 1 to 3 phases), Holo-
150 cene and recent. In the Wind River Range relative and numeric age-dating enable the discrimination

of the following: glacial landforms of Little Ice Age, Black Joe, Alice Lake, Temple Lake, Pinedale, Bull Lake and Sacajawea Ridge stages, and two pre-Sacajawea Ridge deposits that could be attributed to much older glacial events of the mid-late Pleistocene (Dahms, 2004). Thus, in the European Alps, soil chronosequences were available with ages covering a time span of 20 ky and in the Wind River Range with ages extending back to possibly as old as 1.2 Ma.

## 3. Materials and methods

### *3.1. Sampling strategy and soil chemistry/physics*

Soil material was collected from excavated profile pits on undisturbed locations where no influence of creep processes was visible (all on broad moraine crests at Wyoming sites). Although some sites in the Alps were on rather steep slopes, they were fully covered with vegetation and no obvious signs of soil erosion or accumulation were detectable. As soon as a vegetation cover is established in Alpine areas, soil erosion is almost negligible (see also Norton et al., 2010). Profiles were dug to the C horizon when possible. 2-3 kg of soil material per horizon were taken for the analyses (Hitz et al., 2002). The bulk density (fine earth and soil skeleton) was measured using a specific soil core sampler in the Alps and from paraffin-coated peds in the WRR (Dahms, 2002, 2004).

Oven-dried (70°C) samples were sieved to < 2 mm. Fe, Al and Si concentrations were determined after treatment with $NH_4$-oxalate (buffered at pH 3, labelled 'o') (McKeague et al., 1971). The extracts were centrifuged for 8 minutes at 4000 rpm and filtered (mesh size 0.45 µm, S&S, filter type 030/20). Element concentrations were measured using atomic absorption spectroscopy (AAnalyst 700, Perkin Elmer). The oxalate treatment extracts both the weakly- and poorly crystalline phases and some of the organic phases, but normally does not dissolve the strong humus-metal complexes (Mizota and van Reeuwijk, 1989).

175 Measurement of the total element content of fine earth and skeleton was done by means of X-ray
176 fluorescence (XRF). Approximately 10 g of soil material were milled to < 50 µm in a tungsten car-
177 bide disc swing mill (Retsch® RS1, Germany). 4 g of soil powder was mixed with 0.9 g of Li-
178 cowax® C Micro-Powder PM (Clariant, Switzerland), pressed into a 32 mm-pellet and analysed
179 using an energy dispersive X-ray fluorescence spectrometer (SPECTRO X-LAB 2000, SPECTRO
180 Analytical Instruments, Germany). Additional soil chemical and physical characteristics are pre-
181 sented in previous publications (Egli et al., 2001, 2002, 2003, 2010; Dahms, 2002, 2004; Favilli et
182 al., 2009, Böhlert et al., 2011a; Mavris et al., 2010).
183
184 *3.2. Stocks, accumulation and weathering rates*
185 The oxalate-extractable $Fe_o$, $Al_o$, $Si_o$ and $Mn_o$ stocks were calculated according to the following
186 equation:

187 $$Me_{stock} = \sum_{a=1}^{n} Me_i \Delta z_i \rho_i (1 - RM) \qquad (1)$$

188 where $Me_{stock}$ denotes the metal abundance (kg/m$^2$), *Me* the metal concentration (kg/t), $\Delta z_i$ the
189 thickness of layer i (m), $\rho$ = soil density (t/m$^3$) and *RM* the mass proportion of rock fragments.
190 Differences in chemical composition of the parent and soil material can be used to derive weather-
191 ing properties. In most cases, chemical and biophysical weathering is not isovolumetric and the soil
192 volume may dilate or collapse during soil evolution. Using enrichment/depletion amounts deter-
193 mined from concentration profiles of immobile elements such as Ti or Zr, element specific gains
194 and losses are determined and, in the case of known-age landforms, long-term weathering rates are
195 calculated (for theoretical and mathematical background, see Chadwick et al.,1990 and Egli and
196 Fitze, 2000). Volumetric changes assumed to occur during pedogenesis are determined by adopting
197 the classical definition of strain, $\varepsilon_{i,w}$ (Brimhall and Dietrich, 1987):

198 $$\varepsilon_{i,w} = \frac{\Delta z_w}{\Delta z} - 1 \quad \text{or} \quad \varepsilon_{i,w} = \left( \frac{\rho_p C_{j,p}}{\rho_w C_{j,w}} \right) - 1 \qquad (2)$$

199 with $\Delta z$ as the columnar height (m) of a representative initial volume of unweathered parent mate-
200 rial $p$ and $\Delta z_w$ is the weathered equivalent height (m) $w$, $C_{i,p}$ is the concentration of the immobile
201 element $i$ in the parent material (kg/t) and $C_{i,w}$ as the concentration of the immobile element $i$ in
202 weathered product. The calculation of the open-system mass transport function $\tau_{j,w}$ is defined by
203 (Chadwick et al., 1990):

204 $$\tau_{j,w} = \left( \frac{\rho_w C_{j,w}}{\rho_p C_{j,p}} \left( \varepsilon_{i,w} + 1 \right) \right) - 1 \quad \text{or using equation (2)} \quad \tau_{j,w} = \left( \frac{C_{j,w} \cdot C_{i,p}}{C_{i,w} \cdot C_{j,p}} \right) - 1 \qquad (3)$$

205 where $C_{j,p}$ (kg/t) is the concentration of element $j$ in the unweathered parent material, $C_{j,w}$ is the
206 concentration of element $j$ in the weathered product (kg/t), and $\rho_p$ and $\rho_w$ are the bulk density (t/m$^3$)
207 of the parent material and the weathered soil, respectively.
208 This approach is used to calculate the relative element losses of each soil horizon.
209 To estimate the amount of pedogenetically formed $Fe_o$, $Al_o$, $Si_o$ and $Mn_o$ in soils, concentrations of
210 these compounds in the soil column must be compared with the parent material. Using the concept
211 of immobile elements, gains and losses of $Fe_o$, $Al_o$, $Si_o$ and $Mn_o$ can be derived.

212 $$M_{j,w} = Me_{j,w} \left( \frac{\tau_{j,w}}{1 + \tau_{j,w}} \right) \Delta z_w \rho_w (1 - RM) \qquad (4)$$

213 With $n$ soil layers, the mass accumulation of the element $j$ is given by:

214 $$M_{j,w}(\Delta z_w) = \sum_{a=1}^{n} Me_{j,w} \left( \frac{\tau_{j,w}}{1 + \tau_{j,w}} \right) \rho_w (1 - RM) \Delta z_w \qquad (5)$$

215 where $\tau_{j,w}$ corresponds to the mass transport function and $\Delta z$ to the weathered equivalent of the
216 columnar height.
217 Accumulation rates of $Fe_o$, $Al_o$, $Si_o$ and $Mn_o$ are expressed as the amount of pedogenetically formed
218 phases divided by the soil (surface) age ($t$). This gives a production rate $R_{j,w}$ per unit area (equation
219 6).

220 $$R_{j,w} = \frac{M_{j,w}(\Delta z_w)}{t} \qquad (6)$$

For soils developed on bedrock the potential errors are confined to local heterogeneities in bedrock composition. The estimate of the initial composition becomes more difficult when soils are developed on sedimentary parent materials such as loess deposits, debris, or till. For such deposits, the least weathered horizon in the soil profile is assumed to be the parent material. We recognize that soils in glacial deposits often have a certain loess input (e.g., Shroba and Birkeland, 1983; Muhs et al., 1992; Dahms, 1993); however, our present methods cannot quantify loess input to these soils and there is, consequently, some minor error for the quantification of the purely pedogenetically-derived phases.

*3.3. Weathering indexes*

Several indexes have been defined to characterise chemical weathering in soils. The general principle of all these indexes is similar and based on the ratio of the base cations (Ca, Mg, K, Na) to Al and/or Si. We used the 'index B' of Kronberg and Nesbitt (1981) that is defined by the molar ratio:

$$B = \frac{CaO + K_2O + Na_2O}{Al_2O_3 + CaO + K_2O + Na_2O} \quad (7)$$

The molar ratio of (K+Ca)/Ti is used as a 'dating' method for rock varnish in semi-arid to arid regions (Harrington and Whitney, 1987). As Ti is considered to be an immobile element, the ratio can be used as a weathering index: the lower the ratio, the higher the degree of weathering.

*3.4. Statistics*

The individual datasets were checked for normal distribution using a Shapiro-Wilk test (SigmaPlot 11.0 (Systat Software Inc.); Jann, 2005). This procedure was checked using a two-tailed test for significance. The age usually showed a non-normal distribution (even after log-transformation). Consequently, the Spearman rank correlation coefficient was used.

## 4. Results

### *4.1. General characteristics of the soils*

The total elemental content of the fine fraction of the Wind River Range soils is given in Table 3. The analyses confirm the granitic character of all sites. This is expressed by the high $SiO_2$, $Al_2O_3$, $Fe_2O_3$ and low base cation contents.

The average total elemental content of the parent material is given in Table 4. The average composition of the parent material in the Wind River Range does not substantially differ from the parent material composition of the European Alps; although, from a statistical point of view, slight differences are discernible for Mg, K, Fe, Si, P and Mn. From this point of view, similar geochemical conditions exist for all sites.

The oxalate-extractable contents for the Wind River Range soils are given in Table 5. With increasing age, higher concentrations at greater soil depths could usually be measured (although this was not the case for the topsoil). The oxalate-extractable contents for the European Alps were reported previously by Egli et al. (2001, 2002, 2003, 2010), Favilli et al. (2009), Böhlert et al. (2011a) and Mavris et al. (2010). Concentration – depth functions are given in Fig. 2. The concentrations of the oxalate-extractable forms are usually considerably higher in the soils of the Alps than in the WRR. The initial content of $Fe_o$ in the parent material, and to a lesser extent for $Si_o$ and $Al_o$, is higher in the Alps. In contrast to the Wind River Range, there is a pronounced podzolisation effect in the Alps with very low concentrations in the eluvial horizon (where the concentrations dropped almost to zero; Fig. 2).

### *4.2. Mass balance calculations, weathering indexes*

Assuming an increasing element loss with increasing age (a more 'mature' weathering state of the soil), the open-system mass transport function $\tau_{j,w}$ should decrease with increasing soil age. Generally, this is the case. The scatter, however, is relatively high. In Fig. 3, the mean $\tau_{j,w}$ values of Fe

271 and Al and of the base cations (BC) are plotted as a function of time and area (Wind River Range
272 vs. European Alps). Trends with decreasing $\tau_{j,w}$ values in the topsoil as a function of time can be
273 observed. In the European Alps, this decrease is more pronounced pointing to more intense elemen-
274 tal losses (and consequently a higher weathering intensity) over time.
275 As Ti is considered to be an immobile element (White, 1995; Stiles et al., 2003), the (K+Ca)/Ti ra-
276 tio can be used as a weathering index: the lower the ratio, the higher the degree of weathering. The
277 (K+Ca)/Ti ratio in the topsoil (OE, E, A) and subsoil horizons of the Wind River Range showed a
278 slightly significant temporal trend (Fig. 4). A more significant amount of K and Ca is leached with
279 time leading to a passive enrichment of Ti.
280 If not plotted in a logarithmic form (Figs. 3, 4), the open-system mass transport function and the
281 (K+Ca)/Ti ratio both tend to an asymptotic value. The trend for the (K+Ca)/Ti ratio is best ex-
282 pressed using a power law function and the one for $\tau_{j,w}$ using an exponential decay model (see sec-
283 tion 5).
284 The 'index B' (Kronberg and Nesbitt, 1981) is shown (Fig. 5) as a function of time and soil horizon
285 (topsoil and B horizon). For both the Wind River Range and the European Alps, a distinct time
286 trend is present. The slope of the curve for A horizons in the European Alps is slightly steeper than
287 for those in the WRR. The change per unit of time (and thus the reaction rate) also seems to be
288 higher in the Alps. In the B horizon, however, the decreasing tendency of the 'index B' is similar
289 for both regions.
290
291 *4.3. Stocks and accumulation rates of $Fe_o$, $Al_o$, $Si_o$ and $Mn_o$*
292 The pedogenetically formed stocks of $Fe_o$, $Al_o$, $Si_o$ and $Mn_o$ increase considerably with time. This
293 increase seems to be, again, more distinct in the European Alps. In Fig. 6, the total stocks are plot-
294 ted as a function of time together with recently published results of the Damma proglacial area
295 (Dümig et al., 2011). The Damma proglacial area is located in the central Swiss Alps (and conse-

296 quently close to our sites presented in section 2; Fig. 1). As few data are available for very young
297 soils in Alpine areas, the datasets of the Damma proglacial were included.
298 The pedogenic stocks of $Fe_o$, $Al_o$, $Si_o$ and $Mn_o$ are lower than their overall abundance in the profile.
299 No data are available that would have allowed for a calculation of the pedogenic $Fe_o$, $Al_o$, $Si_o$ and
300 $Mn_o$ forms for the Damma proglacial area (as no data about the total elemental content, including
301 immobile elements, were published). The time trend of the pedogenic stocks is similar to the total
302 stock. Using these time trends of pedogenic weakly- and poorly crystalline forms, corresponding
303 formation rates can be derived (Fig. 7). At the beginning of soil formation, these rates are similar in
304 the Wind River Range and European Alps study areas. With time however, the rates seem to de-
305 crease more distinctly at the Wind River Range sites (although the scatter is high for the European
306 Alps).
307
308
309 **5. Discussion**
310 An important requirement for the use of soil chronosequences, including those in glacial forelands,
311 is that the influence of soil-forming factors other than time should be negligible (Jenny, 1941).
312 However, this requirement is often not met (Bardgett et al., 2005) as glacial forelands and, later, the
313 developed soils represent complex and dynamic environments (Anderson, 2007).
314 Despite such shortcomings, distinct trends along the sequences and even some differences between
315 the Wind River Range and the European Alps are seen. As the soil pits were opened at (topographi-
316 cally) stable sites having a similar geochemical composition (parent material) and because the vege-
317 tation cannot be considered as a fully independent state factor, differences between the sites could
318 be attributed predominantly to the factors time and climate.
319 Mass balance calculations, weathering index (‘index B’) and the (K+Ca)/Ti ratio all indicate that
320 significant leaching losses of major base cations have occurred (Fig. 4). These losses led to a corre-

321 sponding passive enrichment of Al or Fe (Martínez Cortizas et al., 2003). The (K+Ca)/Ti ratio re-
322 flects the situation in the topsoils (O, OE and E horizons). Although with a partially high scatter, we
323 can recognize a trend as a function of time. The weathering 'index B' shows a clearer time-trend
324 and thus seems to be a more robust indicator (that does not react too sensitively to local variables).
325 This type of trend is also known from other study areas (Egli et al., 2008). Our results demonstrate
326 that base cation leaching has been the dominant process over the whole observation period. If al-
327 most no disturbances — such as erosion, deposition (or 'upbuilding' according to Johnson et al.
328 (1990)), or pedoturbation — occurred during the life-time of a soil, chronosequences may indicate
329 rates of pedogenic processes (Costantini et al., 2009).
330 Our measured decreases in weathering rates are also supported by laboratory data. White and
331 Brantley (2003) state that the reaction rates of silicate minerals decreases with the duration of
332 chemical weathering. The average silicate weathering rate R (mol $m^{-2}$ $s^{-1}$) was described by a power
333 function $R = 3.1 \times 10^{-13} t^{-0.61}$. Our findings fit this function well, as a power function was found both
334 for our 'index B' and the (K+Ca)/Ti ratio data. Intrinsic surface area, which increases with the dura-
335 tion of weathering, is shown to account for a third of the exponential decrease in the weathering
336 rate. Other factors, including progressive depletion of energetically reactive surfaces and accumula-
337 tion of leached layers and secondary precipitates, contribute to the decrease in weathering rates.
338 Weathering in the topsoil seems to proceed faster in the European Alps. This can be explained by
339 higher precipitation here leading to subsequently higher leaching rates of elements from the soil
340 (see also Egli et al., 2003). The apparent lower weathering rates in moraine soils of the Wind River
341 Range, however, seemed to be slightly influenced by aeolian influx (Dahms, 1993; Dahms and
342 Rawlins, 1996). The influence of loess deposits can be partially inferred by the quantity of silt and
343 clay in A horizons and the mineralogical composition (Dahms, 1993). The dominant minerals in
344 loess are usually quartz (Ollier, 1969; Bronger and Heinkele, 1989), mica and kaolinite giving rise
345 to elemental inputs such as Si, Al and K. The aeolian input is estimated to be in the range of 0.23 to

346 31.0 x $10^{-7}$g $cm^{-2}$ $d^{-1}$ for parts of the Wind River Range (Dahms and Rawlins, 1996). This input of
347 elements slightly affects the trend of the considered weathering indexes and the open-system mass
348 transport function. Furthermore, the loess input also affected the acidity of some soils (Table 5).
349 Despite some differences in the chemistry of the bedrock, distinct trends of Al(o), Fe(o), Si(o) and
350 Mn(o) can be obtained and formation rates of pedogenetically-formed phases can be derived (Fig.
351 6).
352 The chronofunctions of the abundance of weakly- and poorly crystallised phases (pedogenically
353 formed) and of the open mass transport function $\tau_{j,w}$ were best-fitted to data using the exponential
354 decay model. The exponential decay model (cf. Lichter, 1998) is given by:

355 $$f(t) = a + (b - a)e^{-kt} \quad (8)$$

356 where *a* represents an asymptote, *b* the initial quantity, and k the decay constant. This function ex-
357 presses $\frac{dM_s}{dt}$ according to equation 9. We emphasise that any regression model merely approxi-
358 mates reality, and that several models might be equally effective (cf. also Bockheim, 1980; Schaetzl
359 et al., 1994).
360 The abundance and change in abundance per unit area and unit time (formation rates) of the
361 weakly- and poorly crystalline metals ($M_s$) are a function of: the rate at which metals are released
362 from primary minerals ($R_w$), aeolian input ($R_{ae}$), leaching rates in the soil ($L_s$), erosion ($E_s$) and
363 transformation rate of the weakly and poorly crystalline into crystalline forms ($T_s$).
364 This can be described by the following equation:

365 $$\frac{dM_s}{dt} = R_w + R_{ae} - E_s - L_s - T_s \quad (9)$$

366 For Mn, a complete dataset was only available for the Wind River Range. Similar to Fe, Al and Si,
367 however, the rates decrease distinctly (and significantly) as a function of time (Fig. 7). The decrease
368 of the rates fits best with a power law.

With the exponential decay model, a steady state of metal abundances seems to be reached somewhere between 10 and 100 ky. This means that with time $\frac{dM_s}{dt} \approx 0$ and consequently $R_w + R_{ae} \approx E_s + L_s + T_s$. As the increase of metal contents and corresponding abundances can hardly occur endlessly, the decay model is in good agreement with theoretical expectations. For the European Alpine sites, however, no data were available for soils having an age > 30 ky. Consequently, the curve beyond that age is somewhat speculative for these sites and should be verified with additional Alpine sites (having an age of 100 ky and more).

Dorji et al. (2009) found that the detailed picture of a chronosequence can be complicated by minor localised reversals of these trends. It may be that local back-filling and post-incision additions of soil parent material facilitates the persistence of minor peculiarities and apparent inconsistencies.

Pedogenesis through the observed time frame has not been continuous and completely similar at all sites. The study of long-term soil and weathering mechanism signals must, necessarily, cope with such inconveniences (as only natural archives – which includes soils – can give an insight into long-term processes). Although the conditions for soil evolution were not perfectly continuous and identical at all sites, the established sequences are meaningful and give a useful insight into formation rates and soil functions.

## 6. Conclusions

As noted by Böhlert et al. (2011a), the selected parameters (mass balance, weathering indexes) are good parameters that enable an insight into evolutionary processes of the investigated soils. Similar to findings of laboratory experiments (e.g. White and Brantley, 2003), weathering rates in soils decrease with time. Depending on the parameter investigated, a power function ('index B', (K+Ca)/Ti) or an 'exponential decay model function' (accumulation of pedogenically formed weakly- and poorly crystalline phases, τ) best explains the measured trends.

In this study, a data compilation, stock and rate calculation of weakly- and poorly crystallised phases (Fe, Al, Si, Mn) was performed for alpine sites of the Rockies and European Alps. The pedogenically formed, weakly- and poorly crystallised phases were calculated using an approach based on immobile elements. As one of few attempts to date, overall formation rates of these phases are plotted as a function of soil age (and up to ~1 Ma). The formation rates distinctly decrease with increasing age of the soil. This rate of decrease is not only influenced by the factor of time but also by climate (higher precipitation rates lead to a slower rate decrease). These results also suggest that the older soils may be reaching a steady state for these chemical properties in their present environments.

## 7. Acknowledgements

We would like to thank B. Kägi and M. Hilf for the help in the laboratory. We are, furthermore, indebted to two unknown reviewers for their helpful comments on an earlier version of the manuscript.

## References

Alexander, E.B., Burt, R., 1996. Soil development on moraines of Mendenhall Glacier, southeast Alaska. 1. The moraines and soil morphology. Geoderma 72, 1–17.

Anderson, S.P., 2007. Biogeochemistry of glacial landscape systems. Annual Review of Earth and Planetary Science 35, 375–399.

Applegarth, M.T., Dahms, D.E., 2001. Soil catenas of calcareous tills, Whiskey Basin, Wyoming, USA. Catena 42, 17-38.

April, R., Newton, R., Truettner Coles, L., 1986. Chemical weathering in two Adirondack watersheds: past and present-day rates. Geological Society of America Bulletin 97, 1232-1238.

Bain, D.C., Mellor, A., Wilson, M.J., Duthie, D.M.L., 1994. Chemical and mineralogical weathering rates and processes in an upland granitic till catchment in Scotland. Water, Air and Soil Pollution 73, 11 - 27.

Bardgett, R.D., Bowman, W.D., Kaufmann, R., Schmidt, S.K., 2005. A temporal approach to linking aboveground and belowground ecology. Trends in Ecology and Evolution 20, 634–641.

Bernasconi, S.M., Bauder, A., Bourdon, B., Brunner, I., Bünemann, E., Christl, I., Derungs, N., Edwards, P., Farinotti, D., Frey, B., Frossard, E., Furrer, G., Gierga, M., Göransson, H., Gülland, K., Hagedorn, F., Hajdas, I., Hindshaw, R., Ivy-Ochs, S., Jansa, J., Jonas, T., Kicka, M., Kretzschmar, R., Lemarchand, E., Luster, J., Magnusson, J., Mitchell, E.A.D., Olde Venterink, H., Plötze, M., Reynolds, B., Smittenberg, R.H., Stähli, M., Tamburini, F., Tipper, E.T., Wacker, L., Welc, M., Wiederhold, J.G., Zeyer, J., Zimmermann, S., Zumsteg, A., 2011. Chemical and biological gradients along the Damma glacier soil chronosequence, Switzerland. Vadose Zone Journal 10, 867-883.

Birkeland, P.W., 1973. Use of relative age-dating methods in a stratigraphic study of rock glacier deposits, Mt. Sopris, Colorado. Arctic and Alpine Research 5, 401-416.

Birkeland, P.W., 1999. Soils and geomorphology. 3rd edition, Oxford University Press, New York, 430 pp.

Birkeland, P.W., Burke, R.M., Benedict, J.B., 1989. Pedogenic gradients for iron and aluminum accumulation and phosphorus depletion in arctic and alpine soils as a function of time and climate. Quaternary Research 32, 193-204.

Birkeland, P.W., 1984. Soils and Geomorphology. Oxford Univ. Press, NY.

Bockheim, J.G., 1980. Solution and use of chronofunctions in studying soil development. Geoderma 24, 71-85.

443 Böhlert, R., Mirabella, A., Plötze, M., D., Egli, M., 2011a. Landscape evolution in Val Mulix,
444 eastern Swiss Alps – Soil chemical and mineralogical analyses as age proxies. Catena,
445 doi:10.1016/j.catena.2011.06.013.
446 Böhlert, R., Egli, M., Maisch, M. Brandová, D., Ivy-Ochs, S., Kubik, P.W., Haeberli, W. 2011b.
447 Application of a combination of dating techniques to reconstruct the Lateglacial and early Holo-
448 cene landscape history of the Albula region (eastern Switzerland). Geomorphology 127, 1-13.
449 Bohn, H.L., McNeal, B.L., O'Connor, G., 1985. Soil Chemistry. Wiley-Interscience, John Wiley &
450 Sons, New York.
451 Brimhall, G.H., Dietrich, W.E., 1987. Constitutive mass balance relations between chemical com-
452 position, volume, density, porosity, and strain in metasomatic hydrochemical systems: results on
453 weathering and pedogenesis. Geochimica and Cosmochimica Acta 51, 567-587.
454 Bronger, A., Heinkele, T., 1989. Paleosol sequences as witnesses of Pleistocene climatic history. In:
455 Bronger, A., Catt, J.A. (Eds.), Paleopedology – Nature and Applications of Paleosols. Catena
456 Supplement 16, pp. 163-186.
457 Chadwick, O.A., Brimhall, G.H., Hendricks, D.M., 1990. From a black to a grey box - A mass
458 balance interpretation of pedogenesis. Geomorphology 3, 369-390.
459 Costantini, E.A.C., Makeev, A., Sauer, D., 2009. Recent developments and new frontiers in
460 paleopedology. Quaternary International 209, 1-5.
461 Dahms, D.E., 1993. Mineralogical evidence for eolian sediments in soils on Late Quaternary mo-
462 raines, Wind River Mountains, Wyoming. Geoderma 59,175-196.
463 Dahms, D.E., 2002. Glacial Stratigraphy of Stough Creek Basin, Wind River Range, Wyoming.
464 Geomorphology 42, 59-83.
465 Dahms, D.E., 2004. Relative and numeric age data for Pleistocene glacial deposits and diamictons
466 in and near Sinks Canyon, Wind River Range, Wyoming, U.S.A. Arctic, Antarctic, and Alpine
467 Research 36, 59-77.

468 Dahms, D.E., Rawlins, C.L., 1996. A two-year record of eolian sedimentation in the Wind River
469 Range, Wyoming, U.A.A. Arctic and Alpine Research 28, 210-216.
470 Dorji, T., Caspari, T., Bäumler, R., Veldkamp, A., Jongmans, A., Tshering, K., Dorji, T., Baillie, I.,
471 2009. Soil development on Late Quaternary river terraces in a high montane valley in Bhutan,
472 Eastern Himalayas. Catena 78, 48-59.
473 Drever, J.I., 1997. Catchment mass balance. In: Saether O.M., de Caritat, P. (eds), Geochemical
474 Processes, Weathering and Groundwater Recharge in Catchments, Balkema, Rotterdam, pp. 241
475 - 261.
476 Dümig. A., Smittenberg, R., Kögel-Knabner, I., 2011. Concurrent evolution of organic and mineral
477 components during initial soil development after retreat of the Damma glacier, Switzerland. Ge-
478 oderma 163, 83-94
479 Egli, M., Fitze, F., 2000. Formulation of pedoligic mass balance based on immobile elements: a
480 revision. Soil Science 165, 437-443.
481 Egli, M., Fitze, P., Mirabella, A,. 2001. Weathering and evolution of soils formed on granitic,
482 glacial deposits: results from chronosequences of Swiss alpine environments. Catena 45, 19-47.
483 Egli, M., Zanelli, R., Kahr, G., Mirabella, A., Fitze, P. 2002. Soil evolution and development of the
484 clay mineral assemblage of a Podzol and Cambisol in “Meggerwald” (Switzerland). Clay Miner-
485 als 37, 351-366.
486 Egli, M., Mirabella, A., Fitze, P., 2003. Formation rates of smectites derived from two Holocene
487 chronosequences in the Swiss Alps. Geoderma 117, 81-98.
488 Egli, M., Mirabella, A., Nater, M., Alioth, L., Raimondi, S. 2008. Clay minerals, oxyhydroxide
489 formation, element leaching and humus development in volcanic soils. Geoderma 143, 101-114.
490 Egli, M., Brandová, D., Böhlert, R. Favilli, F., Kubik, P., 2010. $^{10}$Be inventories in Alpine soils and
491 their potential for dating land surfaces. Geomorphology 119, 62-73
492 Evans, D.J.A., 1999. A soil chronosequence from neoglacial moraines in western Norway. Geograf-

493 iska Annaler 81A, 47–62.
494 Fabel, D., Harbor, J., Dahms, D., James, A., Elmore, D., Horn, L., Daley, K., Steele, C., 2004. Spa-
495 tial patterns of glacial erosion at a valley scale derived from terrestrial cosmogenic $^{10}$Be and $^{26}$Al
496 concentrations in rock. Annals of the Association of American Geographers 94, 241-255.
497 Favilli, F., Egli, M., Brandová, D., Ivy-Ochs, S., Kubik, P.W., Cherubini, P., Mirabella, A., Sartori,
498 G., Giaccai, D., Haeberli, W. 2009. Combined use of relative and absolute dating techniques for
499 detecting signals of Alpine landscape evolution during the late Pleistocene and early Holocene.
500 Geomorphology 112, 48-66.
501 Fitze, P., 1982. Zur Relativdatierung von Moränen aus Sicht der Bodenentwicklung in den
502 kristallinen Zentralalpen. Catena 9, 265-306.
503 Föllmi, K.B., Arn, K., Hosein, R., Adatte, T., Steinmann, P., 2009a. Biogeochemical weathering in
504 sedimentary chronosequences of the Rhône and Oberaar Glaciers (Swiss Alps): rates and
505 mechanisms of biotite weathering. Geoderma 151, 270-281.
506 Föllmi, K.B., Hosein, R., Arn, K., Steinmann, P., 2009b. Weathering and the mobility of phosphorus
507 in the catchments and forefields of the Rhône and Oberaar glaciers, central Switzerland: Implica-
508 tions for the global phosphorus cycle on glacial-interglacial timescales. Geochimica et Cosmo-
509 chimica Acta 73, 2252-2282.
510 Gile, L.H., Hawley, J.W., Grossman, R.B., 1981. Soils and Geomorphology in the Basin and Range
511 area of Southern New Mexico – Guidebook to the Desert Project. Memoir 39, New Mexico Bu-
512 reau of Mines and Mineral Resources.
513 Hall, R.D., 1999. Effects of climate change on soils in glacial deposits, Wind River Basin, Wyo-
514 ming. Quaternary Research 51, 248-261.
515 Hantke, R., 1983. Eiszeitalter 3: Die jüngste Erdgeschichte der Schweiz und ihrer Nachbargebiete.
516 Westliche Ostalpen mit ihrem bayerischen Vorland bis zum Inn-Durchbruch und Südalpen
517 zwischen Dolomiten und Mont-Blanc. Ott Verlag, Thun, Switzerland.

518 Harrington, C. D., Whitney, J. W., 1987. Scanning electron microscope method of rock-varnish dat-
519 ing. Geology 15, 967-970.
520 Hitz, C., Egli, M., Fitze, P., 2002. Determination of the sampling volume for representative analysis
521 of alpine soils. Zeitschrift für Pflanzenernährung und Bodenkunde 165, 326-331.
522 Hodson, M.E., Langan, S.J., Simon, J., 1999. The influence of soil age on calculated mineral
523 weathering rates. Applied Geochemistry 14, 387– 394.
524 Ivy-Ochs, S., Kerschner, H., Schlüchter, C., 2007. Cosmogenic nuclides and the dating of
525 Lateglacial and Early Holocene glacier variations: The Alpine perspective. Quaternary
526 international 164–165, 53-63.
527 Jann, B., 2005. Einführung in die Statistik. 2., bearbeitete Auflage. München: Oldenburg Wissen-
528 schaftsverlag.
529 Jenny, H. 1941., Factors of Soil Formation. McGraw-Hill, New York.
530 Johnson, D.L., Keller, E.A., Rockwell, T.K., 1990. Dynamic pedogenesis: Niew views on some key
531 soil concepts, and a model for interpreting Quaternary soils. Quaternary Research 33, 306-319.
532 Johnson, W., Lindberg, E., 1992. Atmospheric deposition and forest nutrient cycling: a synthesis of
533 the Integrated Forest Study. Springer Verlag, New York.
534 Keller, O., Krayss, E., 2005. Der Rhein-Linth-Gletscher im Hochglazial. 1. Teil: Einleitung; Aufbau
535 und Abschmelzen des Rhein-Linth-Gletscher im Oberen Würm. Vierteljahresschrift der
536 Naturforschenden Gesellschaft Zürich 150, 19-32.
537 Keller, O., Krayss, E., 1993. The Rhine-Linth Glacier in the upper Würm: A model of the last
538 Alpine glaciation. Quaternary International 18, 15-27.
539 Kronberg, G.I., Nesbitt, H.W., 1981. Quantification of weathering of soil chemistry and soil fertil-
540 ity. Journal of Soil Science 32, 453-459.
541 Lichter, J., 1998. Rates of weathering and chemical depletion in soils across a chronosequence of
542 Lake Michigan sand dunes. Geoderma 85, 255-282.

543 Mahaney, W.C., Hancock, R.G.V., Melville, H., 2011. Late glacial retreat and Neoglacial advance
544 in the Zillertal Alps, Austria. Geomorphology 130, 312-326.
545 Maisch, M., 2000. The longterm signal of climate change in the Swiss Alps: glacier retreat since the
546 end of the little ice age and future decay scenarios. Geografia Fisica e Dinamica Quaternaria 23,
547 139-151.
548 Maisch, M., 1992. Die Gletscher Graubündens: Rekonstruktion und Auswertung der Gletscher und
549 deren Veränderung sit dem Hochstand von 1850 im Gebiet der östlichen Schweizer Alpen
550 (Bündnerland und angrenzende Regionen). Schriftenreihe Physische Geographie 32, Universität
551 Zürich-Irchel, Switzerland.
552 Maisch, M., 1981. Glazialmorphologische und gletschergeschichtliche Untersuchungen im Gebiet
553 zwischen Landwasser- und Albulatal (Kt. Graubünden, Schweiz). Physische Geographie 3.
554 Furrer, G., Keller, W.A., Gamper, M., Suter, J. (Eds). Institute of Geography, University of
555 Zurich.
556 Maisch, M., Brandova, D., Ivy-Ochs, S., Kubik, P.W., 2005. Exposure dating on moraines of the
557 Morteratsch glacier (Bernina region, Upper Engadine, GR). In: Haeberli, W., Giardini, D. (eds.),
558 Proceedings of the 3rd Swiss Geoscience Meeting, Zürich, pp. 181-182.
559 Martínez Cortizas, A., García-Rodeja Gayoso, E., Nóvao Muñoz, J.C., Pontevedra Pombal, X.,
560 Buurman, P., Terribile, F., 2003. Distribution of some selected major and trace elements in four
561 Italian soils developed from the deposits of the Gauro and Vico volcanoes. Geoderma 117, 215-
562 224.
563 Mavris, C., Egli, M., Plötze, M., Blum, J., Mirabella, A., Giaccai, D., Haeberli, W., 2010. Initial
564 stages of weathering and soil formation in the Morteratsch proglacial area (Upper Engadine,
565 Switzerland). Geoderma 155, 359-371.
566 McKeague, J.A., Brydon, J.E., Miles, N.M., 1971. Differentiation of forms of extractable iron and
567 aluminium in soils. Soil Science Society of America Proceedings 35, 33-38.

568 Mizota, C., van Reeuwijk, L.P., 1989. Clay mineralogy and chemistry of soils formed in volcanic
569 material in diverse climat regions. International Soil Reference and Information Centre, Soil
570 Monograph, vol. 2. Wageningen.
571 Muhs, D.R., Benedict, J.B., and Evans, J., 1992. Sources of probable eolian sediments on Late
572 Quaternary alpine moraines, Colorado Front Range: Evidence from trace element geochemistry.
573 Abstract, 12th Biennial meeting, AMQUA, Davis. CA.
574 Munroe, J.S., 2008. Alpine soils on Mount Mansfield, Vermont, USA: Pedology, history and in-
575 traregional comparison. Soil Science Society of America Journal 72, 524-533.
576 Norton, K. P., von Blanckenburg, F., Kubik, P.W., 2010. Cosmogenic nuclide-derived rates of dif-
577 fusive and episodic erosion in the glacially sculpted upper Rhone Valley, Swiss Alps. Earth Sur-
578 face Processes and Landforms 35, 651-662.
579 Ollier, C.D., 1969. Weathering. Oliver & Boyd, Edinburgh, Scotland.
580 Olsson, M.T., Melkerud P.-A., 2000. Weathering in three podzolized pedons on glacial deposits in
581 northern Sweden and central Finland. Geoderma 94, 149-161.
582 Porder, S., Hilley, G.E., Chadwick, O.A., 2007. Chemical weathering, mass loss, and dust inputs
583 across a climate by time matrix in the Hawaiian Islands. Earth and Planetary Science Letters
584 258, 414-427.
585 Riebe, C.S., Kirchner, J.W., Finkel, R.C., 2004. Erosional and climatic effects on long-term chemi-
586 cal weathering rates in granitic landscapes spanning diverse climate regimes. Earth and Planetary
587 Science Letters 224, 547-562.
588 Righi, D., Huber, K., Keller, C., 1999. Clay formation and podzol development from postglacial
589 moraines in Switzerland. Clay minerals 34, 319-332.
590 Ruhe, R.V., Walker, P.H., 1968. Hillslope models and soil formation: II. Closed systems. 9th
591 International Congress of Soil Science (Adelaide, Australia). Transactions Vol 4, 561-568.

592 Sauer, D., Wagner, S., Brückner, H., Scarciglia, F., Mastronuzzi, G., Stahr, K., 2010. Soil
593 development on marine terraces near Metaponto (Gulf of Taranto, southern Italy). Quaternary
594 International 222, 48-63.
595 Scarciglia, F., Pulice, I., Robustelli, G., Vecchio, G., 2006. Soil chronosequences on Quaternary
596 marine terraces along the northwestern coast of Calabria (Southern Italy). Quaternary
597 International 156–157, 133–155.
598 Schaetzl, R.J., Barrett, L.R. and Winkler, J.A., 1994. Choosing models for soil chronofunctions and
599 fitting them to data. European Journal of Soil Science 45, 219-232.
600 Schaller, M., Blum, J.D., Ehlers, T.A., 2009. Combining cosmogenic nuclides and major elements
601 from moraine soil profiles to improve weathering rate estimates. Geomorphology 106, 198-205.
602 Shroba, R.R. and Birkeland, P.W., 1983. Trends in Late Quaternary soil development in the Rocky
603 Mountains and Sierra Nevada of the western United States. In: Wright, H.E. (ed.), Late
604 Quaternary Environments of the United States, Vol 1. The Late Pleistocene. University of
605 Minnesota, Minneapolis, pp. 145-156.
606 Soil Survey Staff, 2010. Keys to Soil Taxonomy, 11$^{th}$ edition. USDA (United States Department of
607 Agriculture), NRCS (National Resources Conservation Service), Washington, DC.
608 Stewart, B.W., Capo, R.C., Chadwick, O.A., 2001. Effects of rainfall on weathering rate, base
609 cation provenance, and Sr isotope composition of Hawaiian soils. Geochimica et Cosmochimica
610 Acta 65, 1087– 1099.
611 Stiles, C.A., Mora, C.I., Driesse, S.G., 2003. Pedogenetic processes and domain boundaries in a
612 Vertisol climosequence: evidence from titanium and zirconium distribution and morphology.
613 Geoderma 116, 279–299.
614 Taylor, A., Blum, J.D., 1995. Relation between soil age and silicate weathering rates determined
615 from the chemical evolution of a glacial chronosequence. Geology 23, 979– 982.
616 Tedrow, J.C.F., 1968. Pedogenic Gradients of the polar regions. Journal of Soil Science 19, 197-

617 204.
618 Tedrow, J.C.F., 1977. Soils of the Polar Landscapes. Rutgers Univ. Press, New Brunswick, N.J.
619 Walker, R.L., del Moral, R., 2003. Primary succession and ecosystem rehabilitation. Cambridge
620 Univ. Press, Cambridge, UK.
621 Walker, L.R., Wardle, D.A., Bardgett, R.D., Clarkson, B.D., 2010. The use of chronosequences in
622 studies of ecological succession and soil development. Journal of Ecology 98, 725–736.
623 White, A.F., 1995. Chemical weathering rates of silicate minerals in soils. In: White, A.F.,
624 Brantley, S.L. (eds), Chemical Weathering Rates of Silicate Minerals. Reviews in Mineralogy,
625 Vol. 31, Mineralogical Society of America, pp. 407-461.
626 White, A.F., Blum, A.E., 1995. Effects of climate on chemical weathering in watersheds.
627 Geochimica et Cosmochimica Acta 59, 1729–1747.
628 White, A.F., Hochella Jr., M.F., 1992. Surface chemistry associated with the cooling and subaerial
629 weathering of resent basalt flows. Geochimica et Cosmochimica Acta 56, 3711 –3721.
630 White, A.F., Brantley, S.L., 2003. The effect of time on the weathering of silicate minerals: why do
631 weathering rates differ in the laboratory and field? Chemical Geology 202, 479-506.
632 Wipf, A., 2001. Gletschergeschichtliche Untersuchungen im spät- und postglazialen Bereich des
633 Hinteren Lauterbrunnentals (Berner Oberland, Schweiz). Geographica Helvetica 56, 133-144.
634 Wright, R.F., Lotse, E., Semb, A., 1994. Experimental acidification of alpine catchments at Sogn-
635 dal, Norway: results after 8 years. Water, Air and Soil Pollution 72, 297 - 315.
636 Zumbühl, H.J., Holzhauser, H., 1988. Alpengletscher in der Kleinen Eiszeit. Die Alpen 64, 129-
637 322.

**Table 1**

Table 1. Characteristics of the Wind River Range sites.

| Site / soil profile | Longitude °E | Latitude °N | Elevation m asl | Aspect °N | Slope % | Slope form* | Parent material | Location | Vegetation | Soils (Soil Taxonomy; Soil Survey Staff, 2010) | Soil age** y | MAP mm/y | MAT °C | Source |
|---|---|---|---|---|---|---|---|---|---|---|---|---|---|---|
| Bigfoot Lake | | | | | | | | | | | | | | |
| 9 | 109° 1'7" | 42°38'12" | 3414 | - | 0 | planar | Granitic till | end moraine | Lichen-covered boulders | Typic Cryorthent | 150 | 800-900 | -3.3 | Dahms, 2002; |
| 6 | 109° 1'4" | 42°38'22" | 3365 | - | 0 | planar | Granitic till | end moraine | Alpine grassland | Typic Haplocryoll | 9930 | 800-900 | -3.0 | |
| 5 | 109° 0'57" | 42°38'22" | 3353 | - | 0 | planar | Granitic till | lateral/end moraine | Alpine grassland | Typic Haplocryoll | 12930 | 800-900 | -2.9 | |
| 1 | 109° 0'39" | 42°38'31" | 3347 | - | 0 | planar | Granitic till | lateral moraine | Alpine grassland | Typic Haplocryoll | 14500 | 800-900 | -2.9 | |
| Stough Creek Basin | | | | | | | | | | | | | | |
| 12 | 109° 0'27" | 42°37'40" | 3475 | - | 0 | planar | Granitic till | end moraine | Alpine grassland | Typic Cryorthent | 1500 | 800-900 | -3.7 | Dahms, 2002 |
| 10 | 108°59'59" | 42°37'58" | 3414 | - | 0 | planar | Granitic till | kame terrace/lateral moraine | Alpine grassland | Typic Haplocryoll | 22000 | 800-900 | -3.3 | |
| Roaring Fork Pass | | | | | | | | | | | | | | |
| 2 | 108°59'58" | 42°39'19" | 3347 | - | 0 | planar | Granitic till | lateral moraine | Alpine grassland | Typic Haplocryoll | 22000 | 800-900 | -2.9 | Dahms, 2002 |
| Pete's Lake Road | | | | | | | | | | | | | | |
| 1 | 108°53'15" | 42°43'40" | 2640 | - | 0 | planar | Granitic till | lateral moraine | Limber pine - common juniper | Ustic Argicryoll | 130000 | 600 | 1.2 | Dahms, 2004; |
| 2 | 108°53'8" | 42°43'36" | 2579 | - | 0 | planar | Granitic till | lateral moraine | Limber pine - common juniper | Ustic Haplocryoll | 22000 | 550 | 1.4 | Fabel et al., 2004 |
| Fairfield Creek | | | | | | | | | | | | | | |
| 5 | 108°51'13" | 42°44'8" | 2329 | - | 0 | planar | Granitic till | lateral moraine | Limber pine, juniper, | Ustic Argicryoll | 65000 | 500 | 2.6 | Dahms, 2004; |

| | | | | | | | | | | | | | | |
|---|---|---|---|---|---|---|---|---|---|---|---|---|---|---|
| | | | | | | | | | sagebrush | | | | | Fabel et al., 2004 |
| 2 | 108°51'29" | 42°44'10" | 2426 | - | 0 | planar | Granitic till | lateral moraine | Limber pine, juniper, sagebrush | Ustic Argicryoll/Palecryoll | 630000 | 500 | 2.0 | |
| Deer Spring | | | | | | | | | | | | | | |
| 1 | 108°48'48" | 42°44'7" | 2304 | - | 0 | planar | Granitic till | lateral moraine | Sagebrush, fescue, wheatgrass | Ustic Argicryoll/Palecryoll | 850000 | 500 | 3.2 | Dahms, 2004; Fabel et al., 2004 |
| Table Mountain | | | | | | | | | | | | | | |
| 1 | 108°45'36" | 42°45'20" | 2225 | - | 0 | planar | Granitic till | unidentified till feature | Sagebrush, fescue, wheatgrass | Ustic Argicryoll/Palecryoll | 1200000 | 450 | 3.4 | Dahms, 2004 |

* perpendicular to slope
** surface age

**Table 2**

Table 2. Characteristics of the Alpine sites.

| Site / soil profile | Longitude °E | Latitude °N | Elevation m asl | Aspect °N | Slope % | Slope form* | Parent material | Location | Vegetation | Soils (Soil taxonomy; Soil Survey Staff, 2010) | Soil age** y | MAP mm/y | MAT °C | Source |
|---|---|---|---|---|---|---|---|---|---|---|---|---|---|---|
| Val di Rabbi | | | | | | | | | | | | | | |
| S1 | 10° 27'36" | 46° 13'42" | 2100 | 60 | 32 | planar | Paragneiss till | Lateral moraine | European larch, common Juniper | Typic Haplocryod | 17311 | 1300 | 1.5 | Favilli et al., 2009 |
| S2 | 10° 27'29" | 46° 13'39 | 2230 | 70 | 55 | planar | Paragneiss till | Lateral moraine | Rhododendron, dwarf shrubs, alpine grassland | Typic Haplocryod | 11106 | 1300 | 0.7 | |
| S3 | 10° 28'34" | 46° 13'30 | 2380 | 320 | 5 | planar | Paragneiss till | Lateral moraine | Alpine grassland | Typic Cryorthent | 10754 | 1300 | 0 | |
| S4 | 10° 28'33" | 46° 13'29 | 2370 | 300 | 10 | planar | Paragneiss till | Solifluction, ground moraine | Alpine grassland | Typic Cryorthent | 8860 | 1300 | 0 | |
| S5 | 10° 27'36" | 46° 13'42 | 2083 | 240 | 32 | concave | Paragneiss till | Lateral moraine | European larch, common Juniper | Typic Haplocryod | 10837 | 1300 | 1.5 | |
| S6 | 10° 27'36" | 46° 13'44 | 2076 | 5 | 38 | planar | Paragneiss till | Lateral moraine | European larch, common Juniper | Typic Haplocryod | 4729 | 1300 | 1.6 | |
| S7 | 10° 27'29" | 46° 13'44 | 2100 | 3 | 43 | planar | Paragneiss till | Lateral moraine | European larch, common Juniper | Typic Haplocryod | 5452 | 1300 | 1.5 | |
| S8 | 10° 26'18" | 46° 13'54 | 2552 | 200 | 33 | concave | Paragneiss till | Inactive rockglacier | Alpine grassland | Humic Dystrocryept | 9203 | 1300 | -1.1 | |
| S9 | 10° 26'20" | 46° 13'48 | 2449 | 90 | 0 | planar | Paragneiss till | Recessional moraine | Alpine grassland | Typic Haplocryod | 11197 | 1300 | -0.4 | |
| Morteratsch | | | | | | | | | | | | | | |
| S1 | 9° 56'39" | 46° 26'49" | 1930 | 330 | 10 | planar | Granitic till | ground moraine | Green alder scrub | Typic Cryorthent | 138 | 1100 | 0.7 | Mavris et al., 2010 |
| S2 | 9° 56'41" | 46° 26'52" | 1930 | | 15 | planar | Granitic till | ground moraine | Green alder scrub | Typic Cryorthent | 128 | 1100 | 0.7 | Egli et al., |

| | | | | | | | | | | | | | | |
|---|---|---|---|---|---|---|---|---|---|---|---|---|---|---|
| S3 | 9° 56'36" | 46° 26'44" | 1930 | 280 | <5 | planar | Granitic till | ground moraine | Epilobietum fleischeri with single willow shrubs and Alpenrose | Typic Cryorthent | 108 | 1100 | 0.7 | 2003; Maisch et al., 2005 |
| S4 | 9° 56'36" | 46° 26'42" | 1935 | 320 | <5 | planar | Granitic till | ground moraine | Epilobietum fleischeri with single willow shrubs and Alpenrose | Typic Cryorthent | 98 | 1100 | 0.7 | |
| S5 | 9° 56'28" | 46° 26'33' | 1950 | 30 | <5 | planar | Granitic till | ground moraine | Pioneer grass communities | Typic Cryorthent | 68 | 1100 | 0.7 | |
| S6 | 9° 56'25" | 46° 26'16' | 2015 | 330 | <5 | planar | Granitic till | ground moraine | Epilobietum fleischeri with single willow shrubs and Alpenrose | Typic Cryorthent | 48 | 1100 | 0.3 | |
| S7 | 9° 56'06" | 46° 26'13" | 2015 | 260 | <5 | planar | Granitic till | ground moraine | Pioneer grass communities | Typic Cryorthent | 48 | 1100 | 0.3 | |
| S8 | 9° 56'07" | 46° 26'20" | 1990 | 150 | <5 | planar | Granitic till | ground moraine | Pioneer grass communities | Typic Cryorthent | 58 | 1100 | 0.5 | |
| S9 | 9° 56'08" | 46° 26'25" | 2000 | 30 | <5 | planar | Granitic till | ground moraine | Pioneer grass communities | Typic Cryorthent | 73 | 1100 | 0.4 | |
| S10 | 9° 56'13" | 46° 26'33" | 1980 | 60 | <5 | planar | Granitic till | ground moraine | Epilobietum fleischeri with single willow shrubs and Alpenrose | Typic Cryorthent | 78 | 1100 | 0.5 | |
| A | 9°56'38" | 46°26'50 | 1930 | 330 | 10 | planar | Granitic till | Lateral moraine | Green alder scrub | Typic Cryorthent | 150 | 1100 | 0.7 | |
| AC | 9°56'27" | 46°26'55" | 1920 | 320 | 10 | convex | Granitic till | Lateral moraine | Larch, Scots pine | Typic Dystrocryept | 1300 | 1100 | 0.8 | |
| AP | 9°57'03" | 46°27'02" | 2030 | 350 | 10 | planar | Granitic till | Lateral moraine | Larch, Scots pine | Typic Haplocryod | 12500 | 1100 | 0.5 | |
| Schmadri | 7°52'36 | 46°30'17" | 2030 | 350 | <5 | planar | Granitic till | Lateral moraine | Alpine grassland | Typic Haplocryod | 3500 | 2000 | 0.5 | Egli et al., 2001; |

| | | | | | | | | | | | | | | |
|---|---|---|---|---|---|---|---|---|---|---|---|---|---|---|
| | 7°52'46" | 46°30'26" | 2020 | 10 | <5 | planar | Granitic till | Lateral moraine | Alpine grassland | Typic Haplocryod | 11500 | 2000 | 0.5 | Wipf, 2001 |
| Val Mulix | | | | | | | | | | | | | | |
| S1 | 9° 44'50" | 46° 34'56" | 2100 | 35 | 11 | planar | Granitic till | Lateral moraine | Larch, Swiss pine, heath | Typic Haplocryod | 14900 | 1250 | -1.1 | Böhlert et al., 2011b; |
| S2 | 9° 45'07" | 46° 34'35" | 2060 | 0 | 16 | planar | Granite | lower rock glacier lobe | Alpine grassland | Typic Haplocryod | 10000 | 1250 | -0.8 | Maisch, 1981 |
| S3 | 9° 45'13" | 46° 34'41" | 2150 | 315 | 9 | planar | Granitic till | Lateral moraine | Alpine grassland | Typic Haplocryod | 10700 | 1250 | -1.3 | |
| S4 | 9° 45'11" | 46° 34'30" | 2130 | 300 | 8 | planar | Granite | middle rock glacier lobe | Alpine grassland | Typic Haplocryod | 9600 | 1250 | -1.2 | |
| S5 | 9° 45'16" | 46° 34'29" | 2280 | 300 | 6 | planar | Granite | upper rock glacier lobe | Alpine grassland | Typic Haplocryod | 8600 | 1250 | -2 | |
| Meggerwald | | | | | | | | | | | | | | |
| | 8°22′17 | 47°03′39" | 620 | 325 | < 10 | planar | Granitic till | ground moraine | White fir, blueberry, European beech | Typic Haplorthod | 19200 | 1300 | 7.5 | Hantke, 1983; Keller and Krayss, 2005; Maisch, 2000; |
| | 8°22′29" | 47°03′31" | 614 | 325 | < 10 | planar | Granitic till | ground moraine | White fir, blueberry, European beech | Spodic Dystrudept | 19200 | 1300 | 7.5 | Egli et al., 2002; Egli et al., 2010 |
| Gletsch | | | | | | | | | | | | | | |
| | 8° 21'52" | 46° 33'53" | 1760 | - | 0 | planar | Granitic till | end moraine | Pioneer grass communities | Typic Udorthent | 150 | 2000 | 1.2 | Egli et al., 2001; |
| | 8° 21'50" | 46° 33'54" | 1760 | - | 0 | planar | Granitic till | end moraine | Pioneer grass communities | Typic Udorthent | 260 | 2000 | 1.2 | Zumbühl and Holzhauser, |
| | 8° 21'46" | 46° 33'52" | 1760 | - | 0 | planar | Granitic till | end moraine | Alpine grassland | Typic Udorthent | 300 | 2000 | 1.2 | 1988 |

| | | | | | | | | | | | | |
|---|---|---|---|---|---|---|---|---|---|---|---|---|
| 8° 21'45" | 46° 33'51" | 1760 | - | 0 | planar | Granitic till | end moraine | Alpine grassland | Typic Dystrudept | 450 | 2000 | 1.2 |
| 8° 21'42" | 46° 33'49" | 1760 | - | 0 | planar | Granitic till | end moraine | Alpine grassland | Typic Dystrudept | 700 | 2000 | 1.2 |
| 8° 21'41" | 46° 33'48" | 1760 | - | 0 | planar | Granitic till | end moraine | Alpine grassland | Typic Dystrudept | 3000 | 2000 | 1.2 |
| 8° 21'23" | 46° 33'40" | 1790 | - | 0 | planar | Granitic till | Lateral moraine | Alpine grassland | Typic Haplorthod | 10500 | 2000 | 1.2 |

* perpendicular to slope
** surface age

**Table 3**

Table 3. Total content (major components; fine earth fraction) of the Wind River Ranges soils.

| Soil | Horizon | Surface age y | Depth cm | $Na_2O$ % | MgO % | $K_2O$ % | CaO % | $Al_2O_3$ % | $Fe_2O_3$ % | $SiO_2$ % | $P_2O_5$ % | MnO % | $TiO_2$ % |
|---|---|---|---|---|---|---|---|---|---|---|---|---|---|
| BFL 9 | Cox | 150 | 0-5 | 3.24 | 2.06 | 2.85 | 3.23 | 13.95 | 4.28 | 62.96 | 0.483 | 0.049 | 0.620 |
| | Cu1 | | 5-15 | 3.31 | 1.79 | 3.03 | 2.95 | 13.82 | 3.94 | 66.06 | 0.476 | 0.041 | 0.581 |
| | Cu2 | | 15-25 | 3.36 | 1.68 | 3.02 | 2.94 | 13.75 | 3.93 | 66.90 | 0.428 | 0.038 | 0.518 |
| SCB 12 | A | 1500 | 0-2 | 3.01 | 2.09 | 3.18 | 3.51 | 13.73 | 4.44 | 63.87 | 0.479 | 0.054 | 0.716 |
| | Cox | | 2-10 | 3.15 | 2.02 | 3.40 | 3.49 | 14.14 | 4.17 | 64.51 | 0.436 | 0.053 | 0.677 |
| | 2Cv | | 10-30 | 3.35 | 1.87 | 3.36 | 3.56 | 14.10 | 4.10 | 66.11 | 0.446 | 0.049 | 0.692 |
| BFL 6 | A | 9930 | 0-10 | 1.80 | 2.15 | 2.43 | 3.06 | 11.69 | 3.75 | 51.38 | 0.518 | 0.076 | 0.615 |
| | 2Bt | | 10-20 | 2.44 | 2.15 | 2.63 | 2.79 | 13.93 | 3.92 | 58.37 | 0.347 | 0.046 | 0.539 |
| | 2Cox1 | | 20-28 | 2.49 | 1.79 | 2.67 | 2.48 | 12.91 | 3.31 | 58.39 | 0.216 | 0.037 | 0.534 |
| | 2Cox2 | | 28-45 | 2.82 | 2.39 | 2.32 | 3.25 | 14.17 | 4.44 | 61.87 | 0.257 | 0.051 | 0.590 |
| BFL 5 | A 0-9 | 12930 | 0-9 | 2.17 | 1.81 | 2.76 | 2.29 | 12.35 | 3.46 | 55.41 | 0.448 | 0.053 | 0.560 |
| | 2Bt | | 9-22 | 2.32 | 2.41 | 2.82 | 2.27 | 13.42 | 4.20 | 56.92 | 0.536 | 0.049 | 0.683 |
| | 2Cox1 | | 22-55 | 1.85 | 2.85 | 2.68 | 2.40 | 15.52 | 4.76 | 65.25 | 0.296 | 0.045 | 0.752 |
| | 2Cox2 | | 55-75 | 3.75 | 1.81 | 3.37 | 1.73 | 13.79 | 3.23 | 67.14 | 0.305 | 0.028 | 0.555 |
| BFL 1 | A | 14500 | 0-8 | 1.63 | 1.94 | 2.58 | 2.36 | 12.08 | 3.49 | 51.82 | 0.599 | 0.073 | 0.639 |
| | Bt | | 8-18 | 2.29 | 1.84 | 2.53 | 2.35 | 13.88 | 3.71 | 58.81 | 0.468 | 0.049 | 0.585 |
| | 2BC | | 18-28 | 3.34 | 1.51 | 3.09 | 2.80 | 13.93 | 3.28 | 66.48 | 0.373 | 0.038 | 0.525 |
| | 2Cox1 | | 27-65 | 2.89 | 2.20 | 3.04 | 2.72 | 14.60 | 4.22 | 62.27 | 0.304 | 0.047 | 0.671 |
| | 2Cox2 | | 65-90 | 3.18 | 2.23 | 3.12 | 3.09 | 13.98 | 4.44 | 64.04 | 0.436 | 0.050 | 0.711 |
| SCB 10 | A | 16000 | 0-6 | 1.05 | 2.00 | 1.65 | 2.35 | 9.09 | 4.08 | 35.92 | 0.471 | 0.059 | 0.672 |
| | Ej | | 6-7 | 1.31 | 2.39 | 1.88 | 2.24 | 11.13 | 5.14 | 42.31 | 0.492 | 0.041 | 0.907 |
| | Bw | | 7-11 | 1.37 | 1.69 | 1.74 | 2.05 | 10.50 | 3.99 | 43.32 | 0.612 | 0.029 | 0.646 |
| | 2ABb | | 11-23 | 2.09 | 1.73 | 2.01 | 2.14 | 12.40 | 4.02 | 52.80 | 0.585 | 0.035 | 0.633 |
| | 2Btb | | 23-29 | 3.31 | 1.73 | 2.08 | 2.72 | 14.33 | 4.18 | 60.87 | 0.311 | 0.036 | 0.687 |
| | 3Cox1b | | 29-75 | 3.96 | 1.44 | 2.27 | 3.17 | 14.62 | 4.20 | 65.45 | 0.388 | 0.032 | 0.545 |

| | | | | | | | | | | | | | |
|---|---|---|---|---|---|---|---|---|---|---|---|---|---|
| | 3Cox2b | | 75-85 | 3.70 | 1.62 | 2.43 | 3.00 | 14.75 | 4.77 | 63.91 | 0.334 | 0.036 | 0.629 |
| RFP 2 | A | 16000 | 0-13 | 1.31 | 1.76 | 2.06 | 1.83 | 11.63 | 3.60 | 50.41 | 0.485 | 0.082 | 0.610 |
| | 2Bt1 | | 13-23 | 2.37 | 2.56 | 2.11 | 2.14 | 14.14 | 4.75 | 59.83 | 0.225 | 0.046 | 0.645 |
| | 2Bt2 | | 23-50 | 2.70 | 2.53 | 2.15 | 2.44 | 13.79 | 4.96 | 59.64 | 0.210 | 0.055 | 0.642 |
| | 2BC | | 50-60 | 3.20 | 2.15 | 2.43 | 2.47 | 14.65 | 4.41 | 62.95 | 0.260 | 0.054 | 0.564 |
| | 2Cox | | 60-75 | 3.28 | 2.24 | 2.32 | 2.59 | 14.77 | 4.61 | 62.15 | 0.265 | 0.055 | 0.602 |
| PLR 2 | A | 22000 | 0-10 | 2.56 | 1.29 | 2.77 | 2.51 | 13.57 | 3.91 | 62.95 | 0.344 | 0.063 | 0.536 |
| | AB | | 10-20 | 2.90 | 1.21 | 2.80 | 2.54 | 13.96 | 3.84 | 64.46 | 0.326 | 0.051 | 0.582 |
| | BW | | 20-30 | 3.20 | 1.12 | 2.81 | 2.75 | 13.95 | 4.67 | 67.36 | 0.311 | 0.036 | 0.616 |
| | Cox | | 30-50 | 2.60 | 1.27 | 2.57 | 2.89 | 13.77 | 3.74 | 62.72 | 0.322 | 0.027 | 0.550 |
| | 2C | | > 50 | 2.14 | 1.27 | 2.49 | 2.78 | 12.13 | 3.89 | 56.60 | 0.259 | 0.030 | 0.567 |
| FC5 | A | 65000 | 0-7 | 1.43 | 1.27 | 2.16 | 3.28 | 9.90 | 3.30 | 47.58 | 0.356 | 0.052 | 0.571 |
| | Bt1 | | 7-25 | 2.52 | 1.32 | 2.62 | 2.76 | 13.00 | 3.73 | 62.14 | 0.305 | 0.035 | 0.612 |
| | 2Bt2 | | 25-50 | 3.07 | 1.24 | 2.82 | 2.84 | 13.38 | 3.75 | 64.51 | 0.274 | 0.027 | 0.502 |
| | 2Coxx | | 50-85 | 3.17 | 1.16 | 2.66 | 2.88 | 13.14 | 3.57 | 66.87 | 0.248 | 0.028 | 0.514 |
| | 2C | | > 85 | 3.49 | 0.97 | 2.74 | 2.88 | 13.21 | 3.33 | 69.21 | 0.213 | 0.024 | 0.444 |
| PLR1 | A | 130000 | 0-8 | 1.31 | 1.58 | 2.58 | 1.71 | 12.57 | 3.70 | 65.29 | 0.325 | 0.086 | 0.649 |
| | Bt1b | | 8-30 | 1.30 | 1.63 | 2.45 | 1.53 | 12.63 | 4.08 | 66.49 | 0.272 | 0.068 | 0.702 |
| | Bt2b | | 30-50 | 1.27 | 1.66 | 2.43 | 1.46 | 12.74 | 4.01 | 69.16 | 0.242 | 0.064 | 0.700 |
| | Bt3b | | 50-85 | 0.87 | 1.98 | 2.10 | 1.27 | 12.89 | 4.06 | 67.82 | 0.180 | 0.059 | 0.678 |
| | 2Coxb | | 85-100 | 2.07 | 1.90 | 2.46 | 2.32 | 13.12 | 4.57 | 63.30 | 0.272 | 0.048 | 0.713 |
| FC2 | A | 630000 | 3-5 | 1.09 | 1.58 | 2.93 | 2.07 | 12.32 | 3.08 | 54.42 | 0.356 | 0.057 | 0.530 |
| | Bt1 | | 5-23 | 1.30 | 1.71 | 2.83 | 1.57 | 14.05 | 3.08 | 55.10 | 0.224 | 0.032 | 0.472 |
| | 2Bt2b | | 23-45 | 1.24 | 1.78 | 3.36 | 1.44 | 14.67 | 2.67 | 61.54 | 0.110 | 0.019 | 0.376 |
| | 2Coxb | | 130-210 | 1.25 | 1.88 | 2.65 | 1.59 | 13.54 | 2.67 | 60.82 | 0.083 | 0.015 | 0.346 |
| | 2Cb | | > 210 | 1.24 | 2.02 | 2.68 | 1.75 | 13.77 | 3.98 | 60.19 | 0.142 | 0.025 | 0.436 |
| DS1 | A | 850000 | 0-11 | 1.02 | 1.83 | 3.11 | 1.67 | 14.71 | 3.92 | 57.57 | 0.265 | 0.069 | 0.731 |
| | Btb1 | | 11-30 | 1.12 | 2.15 | 2.76 | 1.74 | 15.48 | 3.94 | 58.03 | 0.184 | 0.041 | 0.593 |
| | 2Bt2b | | 30-150 | 0.74 | 2.50 | 2.53 | 1.98 | 15.41 | 2.67 | 55.43 | 0.106 | 0.021 | 0.411 |
| TM-1 | A | 1200000 | 0-12 | 1.60 | 1.68 | 2.45 | 2.23 | 16.77 | 5.67 | 53.82 | 0.318 | 0.045 | 0.834 |

| | | | | | | | | | | | |
|---|---|---|---|---|---|---|---|---|---|---|---|
| B | 12-20 | 1.60 | 1.38 | 2.72 | 2.09 | 15.71 | 5.00 | 55.18 | 0.238 | 0.039 | 0.743 |
| Bt1b1 | 20-45 | 1.51 | 1.53 | 2.38 | 2.16 | 16.57 | 5.42 | 54.32 | 0.245 | 0.042 | 0.807 |
| Bt2b1 | 45-60 | 1.58 | 1.54 | 2.44 | 2.21 | 16.56 | 5.47 | 53.80 | 0.268 | 0.044 | 0.792 |
| Coxb1 | 65-85 | 1.67 | 1.41 | 2.66 | 2.07 | 16.18 | 5.09 | 55.12 | 0.237 | 0.044 | 0.785 |
| ABb2 | 85-115 | 1.38 | 1.59 | 2.51 | 2.16 | 15.12 | 4.99 | 52.70 | 0.298 | 0.048 | 0.703 |
| Bt1b2 | 115-150 | 1.18 | 1.69 | 2.79 | 1.67 | 14.33 | 4.50 | 57.21 | 0.179 | 0.034 | 0.655 |
| Bt2b2 | 150-200 | 1.45 | 1.54 | 2.91 | 1.87 | 15.45 | 5.08 | 54.90 | 0.152 | 0.026 | 0.641 |
| Bt3b2 | 200-300 | 1.24 | 1.62 | 2.82 | 1.77 | 15.22 | 5.23 | 55.49 | 0.140 | 0.027 | 0.731 |
| Cox1b2 | 300-400 | 1.65 | 1.54 | 1.95 | 2.79 | 16.22 | 3.92 | 55.23 | 0.153 | 0.017 | 0.678 |
| Cox2b2 | 400-500 | 1.38 | 1.51 | 2.77 | 1.69 | 16.29 | 4.78 | 55.36 | 0.108 | 0.026 | 0.644 |

**Table 4**

Table 4. Average composition (major inorganic compounds) of the parent material (fine earth) of both investigation regions.

| | $Na_2O$ (%) | MgO (%) | $K_2O$ (%) | CaO (%) | $Al_2O_3$ (%) | $Fe_2O_3$ (%) | $SiO_2$ (%) | $P_2O_5$ (%) | MnO (%) | $TiO_2$ (%) |
|---|---|---|---|---|---|---|---|---|---|---|
| Alps (n=30) | | | | | | | | | | |
| Average | 3.01 | 1.07 | 3.58 | 0.98 | 13.80 | 3.17 | 66.92 | 0.128 | 0.055 | 0.762 |
| SD | 0.98 | 0.67 | 0.74 | 0.61 | 2.81 | 1.90 | 6.59 | 0.030 | 0.027 | 0.450 |
| Median | 3.11 | 0.99 | 3.51 | 0.93 | 14.48 | 2.77 | 67.18 | 0.13 | 0.053 | 0.805 |
| Wind River Range (n = 22) | | | | | | | | | | |
| Average | 2.73 | 1.79 | 2.73 | 2.68 | 14.09 | 4.03 | 62.92 | 0.290 | 0.037 | 0.589 |
| SD | 0.85 | 0.44 | 0.38 | 0.57 | 1.01 | 0.56 | 3.88 | 0.113 | 0.012 | 0.102 |
| Median | 3.02 | 1.80* | 2.68* | 2.83 | 13.90 | 4.04* | 63.60* | 0.28* | 0.036* | 0.586 |

*Differences between the Alps and the Wind River Range are significant based on the Mann-Whitney test

**Table 5**

Table 5. Concentrations of oxalate-extractable Fe, Al, Si and Mn (fine earth), pH and some physical properties of the Wind River Range soils

| Surface age (y) | Soil | Horizon | Depth (cm) | Layer (cm) | Gravel-w% | Bulk density ($g/cm^3$) | pH ($CaCl_2$) | Fe (mg/kg) | Mn (mg/kg) | Si (mg/kg) | Al (mg/kg) |
|---|---|---|---|---|---|---|---|---|---|---|---|
| 150 | BFL 9 | Cox | 0-5 | 5 | 42 | 1.35 | 4.6 | 1055 | 47 | 259 | 476 |
| | | Cu1 | 5-15 | 10 | 56 | 1.77 | 4.5 | 1014 | 39 | 110 | 304 |
| | | Cu2 | 15-25 | 10 | 56 | 1.77 | 4.5 | 784 | 27 | 49 | 195 |
| 1500 | SCB 12 | A | 0-2 | 2 | 31 | 1.35 | 4.9 | 1978 | 72 | 379 | 739 |
| | | Cox | 2-10 | 8 | 47 | 1.77 | 4.9 | 856 | 49 | 366 | 444 |
| | | 2Cu | 10-30 | 20 | 51 | 1.77 | 4.9 | 885 | 34 | 272 | 379 |
| 9930 | BFL 6 | A | 0-10 | 10 | 7 | 0.98 | 5.3 | 1598 | 246 | 112 | 1298 |
| | | 2Bt | 10-20 | 10 | 29 | 1.20 | 5.1 | 663 | 13 | 9 | 845 |
| | | 2Cox1 | 20-28 | 8 | 34 | 1.54 | | 259 | 4 | 18 | 183 |
| | | 2Cox2 | 28-45 | 17 | 33 | 1.77 | 4.7 | 259 | 4 | 18 | 183 |
| 12930 | BFL 5 | A 0-9 | 0-9 | 9 | 22 | 0.94 | 5.2 | 1100 | 77 | 128 | 1320 |
| | | 2Bt | 9-22 | 13 | 31 | 1.26 | 4.7 | 498 | 32 | 139 | 1728 |
| | | 2Cox1 | 22-55 | 33 | 32 | 1.62 | 4.4 | 338 | 6 | 42 | 385 |
| | | 2Cox2 | 55-75 | 20 | 46 | 1.77 | 4.5 | 143 | 2 | 14 | 68 |
| 14500 | BFL 1 | A | 0-8 | 8 | 8 | 1.21 | 5.2 | 809 | 106 | 190 | 2025 |
| | | Bt | 8-18 | 10 | 20 | 1.27 | 4.9 | 795 | 43 | 193 | 2403 |
| | | 2BC | 18-28 | 10 | 40 | 1.32 | 5.0 | 431 | 11 | 83 | 508 |
| | | 2Cox1 | 27-65 | 38 | 43 | 1.45 | 4.6 | 598 | 9 | 68 | 505 |
| | | 2Cox2 | 65-90 | 25 | 53 | 1.77 | 4.7 | 576 | 10 | 62 | 188 |
| 16000 | SCB 10 | A | 0-6 | 6 | 3 | 0.96 | 4.4 | 2275 | 161 | 81 | 1784 |
| | | Ej | 6-7 | 1 | 3 | 1.10 | | 2871 | 19 | 108 | 2153 |
| | | Bw | 7-11 | 4 | 4 | 0.97 | 4.0 | 2437 | 13 | 90 | 2211 |
| | | 2ABb | 11-23 | 12 | 17 | 1.01 | 4.0 | 1969 | 27 | 75 | 2334 |

| | | | | | | | | | | | |
|---|---|---|---|---|---|---|---|---|---|---|---|
| | | 2Btb | 23-29 | 6 | 22 | 1.20 | 4.2 | 949 | 19 | 35 | 1116 |
| | | 3Cox1b | 29-75 | 46 | 37 | 1.54 | 4.5 | 220 | 4 | 5 | 314 |
| | | 3Cox2b | 75-85 | 10 | 46 | 1.77 | 4.3 | 210 | 13 | 25 | 746 |
| 16000 | RFP 2 | A | 0-13 | 13 | 6 | 1.03 | 4.4 | 3327 | 448 | 168 | 2787 |
| | | 2Bt1 | 13-23 | 10 | 17 | 1.17 | 4.2 | 1804 | 9 | 83 | 1732 |
| | | 2Bt2 | 23-50 | 27 | 35 | 1.34 | 4.2 | 1856 | 13 | 98 | 1716 |
| | | 2BC | 50-60 | 10 | 33 | 1.54 | 4.2 | 523 | 25 | 34 | 2701 |
| | | 2Cox | 60-75 | 15 | 42 | 1.77 | 4.2 | 633 | 28 | 454 | 3141 |
| 22000 | PLR 2 | A | 0-10 | 10 | 20.5 | 1.26 | 5.1 | 2383 | 331 | 67 | 1582 |
| | | AB | 10-20 | 10 | 23.1 | 1.35 | 5.2 | 1205 | 179 | 84 | 972 |
| | | BW | 20-30 | 10 | 40.7 | 1.45 | 5.1 | 2253 | 70 | 84 | 646 |
| | | Cox | 30-50 | 20 | 41.6 | 1.77 | 5.3 | 267 | 15 | 16 | 360 |
| | | 2C | > 50 | 10 | 52.8 | 1.83 | 5.4 | 746 | 12 | 21 | 290 |
| 65000 | FC5 | A | 0-7 | 7 | 16.2 | 1.26 | 5.3 | 1366 | 131 | 67 | 691 |
| | | Bt1 | 7-25 | 18 | 27.3 | 1.54 | 5.4 | 1831 | 67 | 105 | 606 |
| | | 2Bt2 | 25-50 | 25 | 26.3 | 1.59 | 5.6 | 1810 | 18 | 79 | 375 |
| | | 2Coxx | 50-85 | 35 | 32.5 | 1.77 | 5.6 | 235 | 27 | 23 | 262 |
| | | 2C | > 85 | 10 | 39.6 | 1.83 | 5.8 | 1041 | 20 | 44 | 165 |
| 130000 | PLR1 | A | 0-8 | 8 | 18.4 | 1.26 | 5.3 | 2240 | 415 | 175 | 1145 |
| | | Bt1b | 8-30 | 22 | 16.5 | 1.54 | 5.3 | 1795 | 287 | 137 | 1039 |
| | | Bt2b | 30-50 | 20 | 12.4 | 1.59 | 5.3 | 1530 | 241 | 123 | 999 |
| | | Bt3b | 50-85 | 35 | 7.5 | 1.59 | 5.5 | 1326 | 256 | 145 | 1164 |
| | | 2Coxb | 85-100 | 15 | 53.1 | 1.77 | 5.5 | 666 | 89 | 56 | 477 |
| 630000 | FC2 | A | 3-5 | 5 | 20.8 | 1.07 | 5.6 | 1636 | 202 | 139 | 1386 |
| | | Bt1 | 5-23 | 18 | 18.1 | 1.41 | 5.3 | 507 | 59 | 58 | 695 |
| | | 2Bt2b | 23-45 | 107 | 16.8 | 1.58 | 5.5 | 320 | 26 | 60 | 664 |
| | | 2Coxb | 130-210 | 80 | 14.1 | 1.77 | 6.0 | 82 | 1 | 49 | 294 |
| | | 2Cb | > 210 | 10 | 7.7 | 1.83 | 6.0 | 123 | 1 | 70 | 447 |

| | | | | | | | | | | | |
|---|---|---|---|---|---|---|---|---|---|---|---|
| 850000 | DS1 | A | 0-11 | 11 | 14.5 | 1.31 | 5.5 | 1415 | 219 | 126 | 1144 |
| | | Btb1 | 11-30 | 19 | 20.1 | 1.47 | 5.4 | 732 | 99 | 99 | 1329 |
| | | 2Bt2b | 30-150 | 120 | 36.2 | 1.53 | 5.5 | 136 | 12 | 55 | 738 |
| 1200000 | TM-1 | A | 0-12 | 12 | 0.0 | 1.26 | 6.4 | 554 | 97 | 105 | 368 |
| | | B | 12-20 | 8 | 0.7 | 1.83 | 6.5 | 519 | 75 | 92 | 282 |
| | | Bt1b1 | 20-45 | 15 | 0.0 | 1.54 | 6.2 | 488 | 86 | 91 | 312 |
| | | Bt2b1 | 45-60 | 15 | 2.0 | 1.59 | 6.0 | 563 | 106 | 102 | 347 |
| | | Coxb1 | 65-85 | 20 | 1.2 | 1.77 | 5.9 | 737 | 105 | 104 | 432 |
| | | ABb2 | 85-115 | 30 | 5.2 | 1.26 | 6.2 | 1028 | 131 | 118 | 700 |
| | | Bt1b2 | 115-150 | 35 | 17.9 | 1.54 | 6.0 | 581 | 73 | 75 | 756 |
| | | Bt2b2 | 150-200 | 50 | 18.4 | 1.54 | 5.7 | 188 | 20 | 61 | 450 |
| | | Bt3b2 | 200-300 | 100 | 11.6 | 1.59 | 5.8 | 265 | 43 | 80 | 457 |
| | | Cox1b2 | 300-400 | 100 | 18.5 | 1.77 | 6.1 | 174 | 35 | 64 | 367 |
| | | Cox2b2 | 400-500 | 100 | 16.1 | 1.77 | 6.0 | 228 | 39 | 65 | 241 |

## Figure captions

Fig. 1. Location of the study sites (data source and imagery: Harris Corp, Earthstar Geographic LLC; sci Lands – scientific landscapes, Göttingen). European Alps: VdR = Val di Rabbi, M = Morteratsch, Sc = Schmadri, VM = Val Mulix, MW = Meggerwald, Gl = Gletsch; Wind River Range: BFL =Bigfoot Lake, SCB = Stough Creek Basin, RFP = Roaring Fork Pass, PLR = Pete's Lake Road, FC = Fairfield Creek, DS = Deer Spring, TM = Table Mountain.

Fig. 2. Concentration – depth function for the oxalate-extractable Fe (Wind River Range and European Alps) and Mn (only Wind River Range). The soil profiles are classified according to their surface age.

Fig. 3. Time trend of the open mass transfer function $\tau_{j,w}$ (mean value) in the topsoil for the base cations (BC: Ca, Mg, K, Na) and Fe and Al. The trend is modelled using an exponential decay model (see equation 8). The fitting parameters are for BC: Wind River Range (a = -0.22; b = 0; k = 0.000091), Alps (a = -0.62; b = 0; k = 0.000094) and for Al + Fe: Wind River Range (a = -0.22; b = 0; k = 0.000092), Alps (a = -0.61; b = 0; k = 0.000102).

Fig. 4. (K+Ca)/Ti ratio in the topsoil and in the B horizon of the Wind River Range as a function of time.

Fig. 5. Weathering index B (according to Kronberg and Nesbitt, 1981) in the topsoil and in the B horizon for the Wind River Range and the Alps as a function of time.

Fig. 6. A) Total stocks of oxalate-extractable Fe, Al and Si (including the sites of the proglacial area Damma; Dümig et al., 2011) and B) pedogenetically formed abundances of Fe, Al, Si and Mn as a function of time (without the proglacial area Damma due to missing data). The Pedogenetic stocks of Fe, Al, Si and Mn were calculated according to the equations 4-6. The trend for the pedogenetically forms is modelled using an exponential decay model (see equation 9). WRR = Wind River Range.

Fig. 7. Accumulation rates of pedogenetically formed Fe, Al, Si and Mn forms (for Mn: data is only available for the Wind River Range).

Figure 1

Click here to download high resolution image

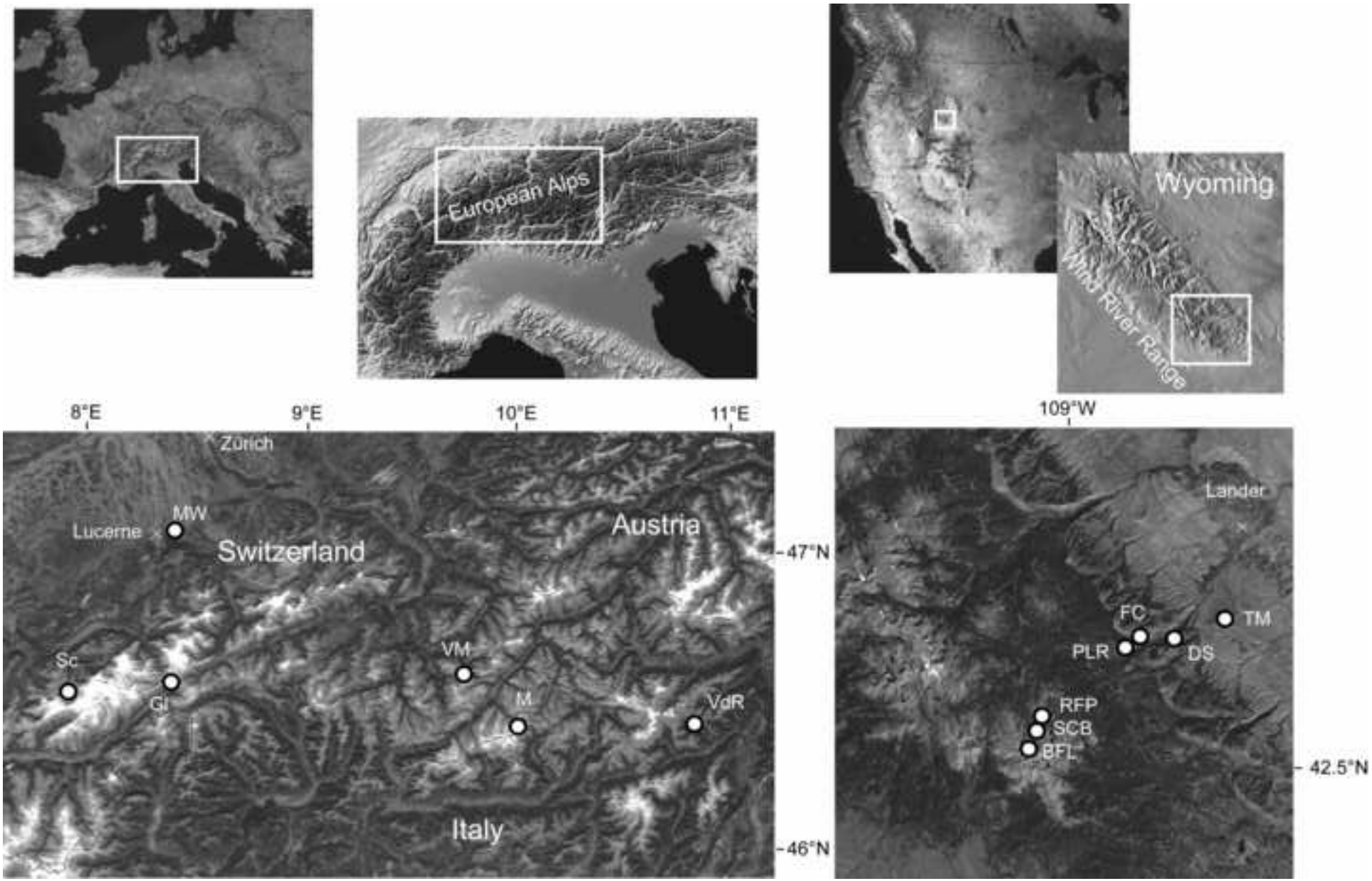

**Figure 2**

**Click here to download high resolution image**

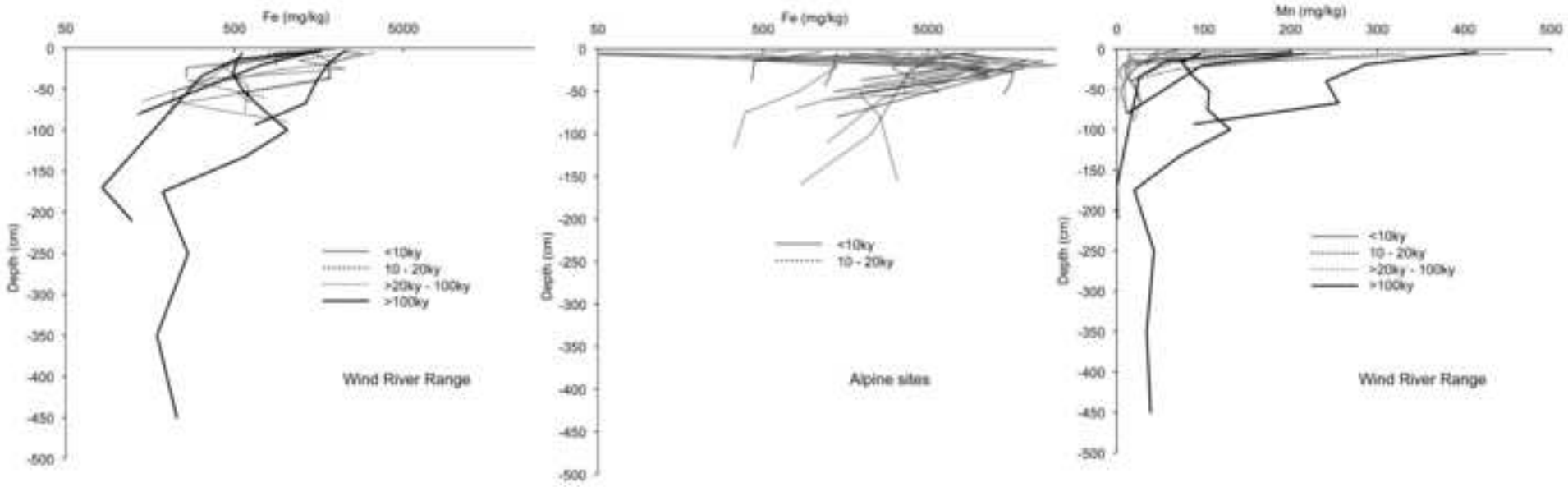

**Figure 3**

**Click here to download high resolution image**

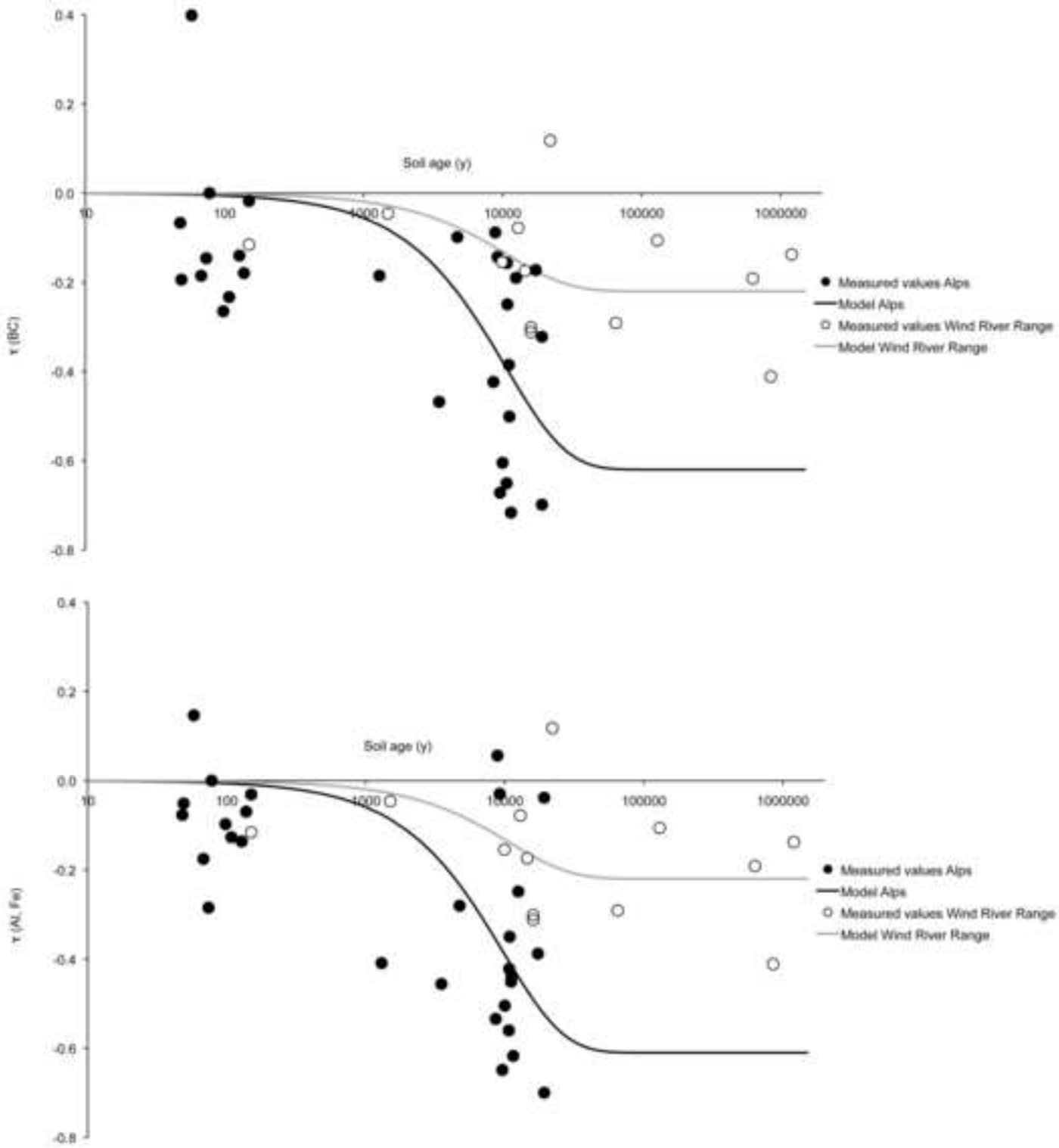

**Figure 4**

Click here to download high resolution image

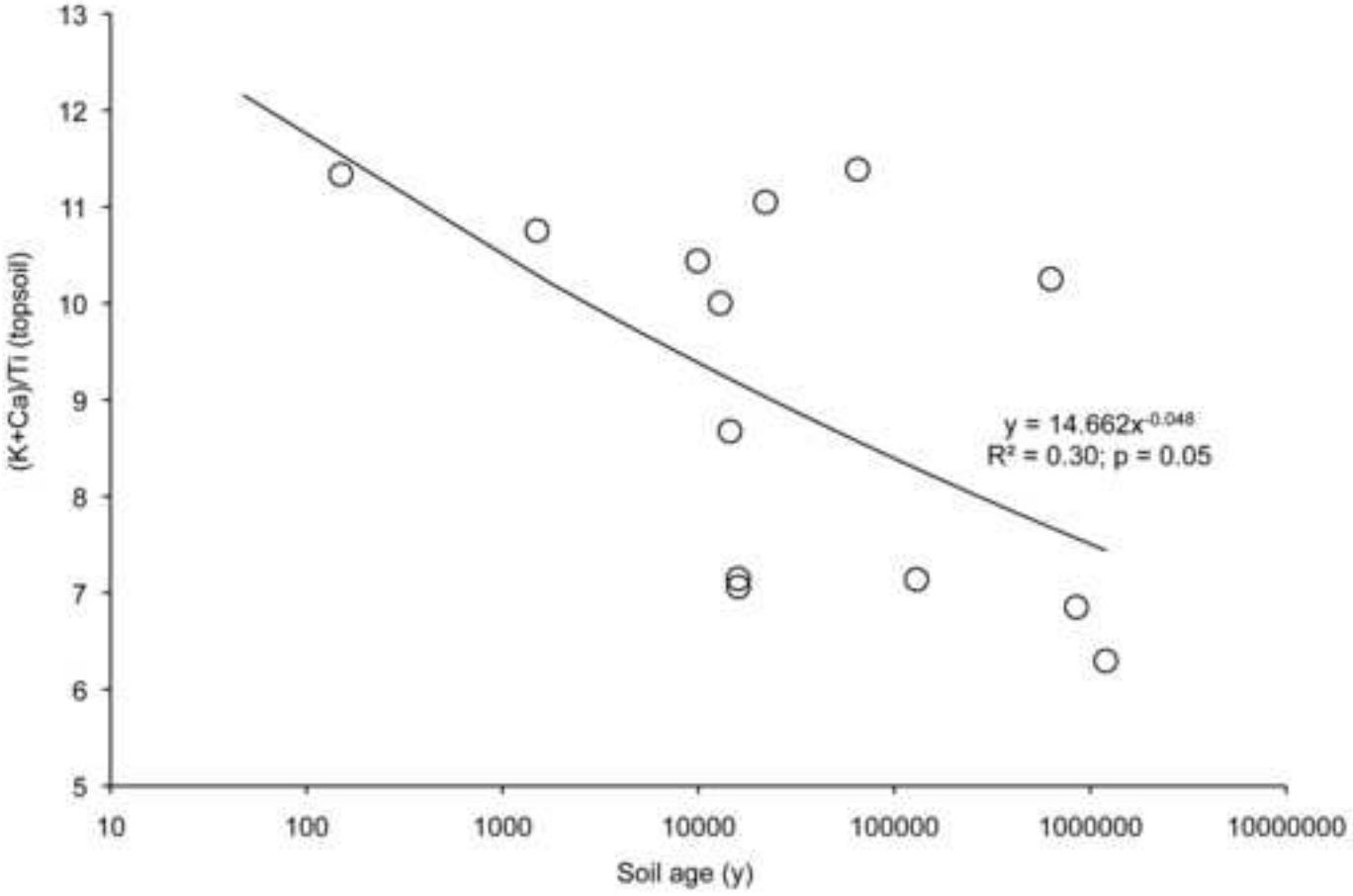


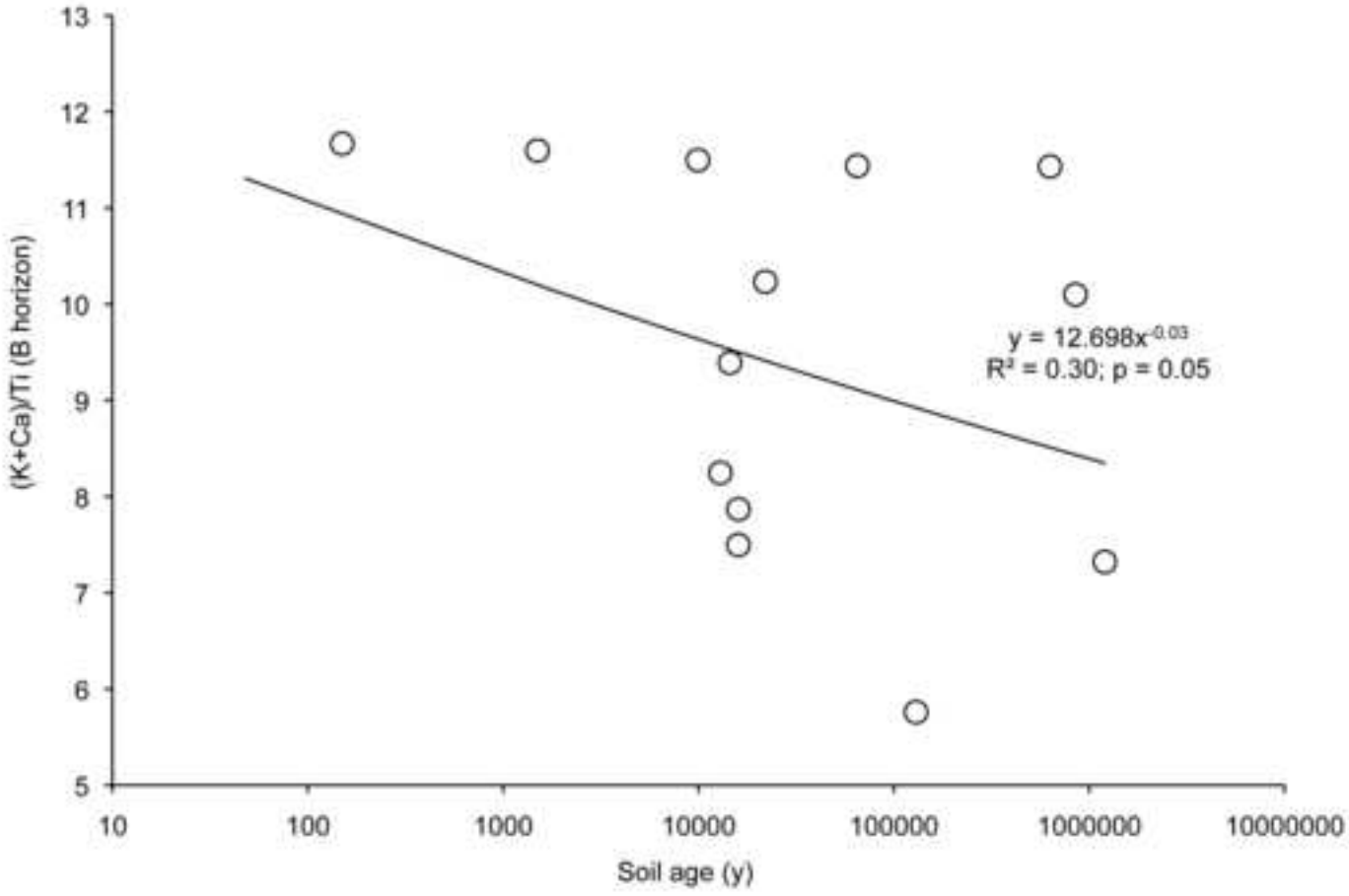

**Figure 5**

Click here to download high resolution image

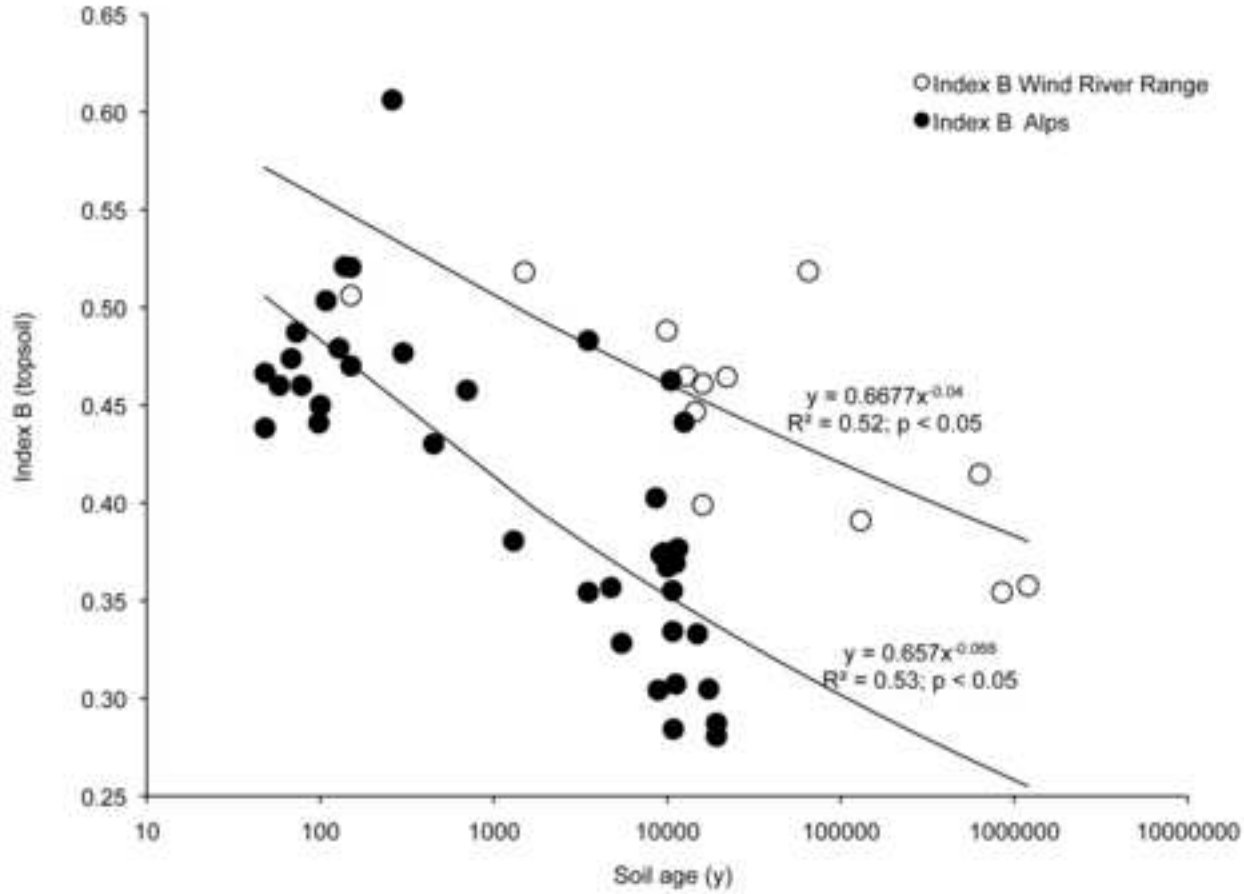


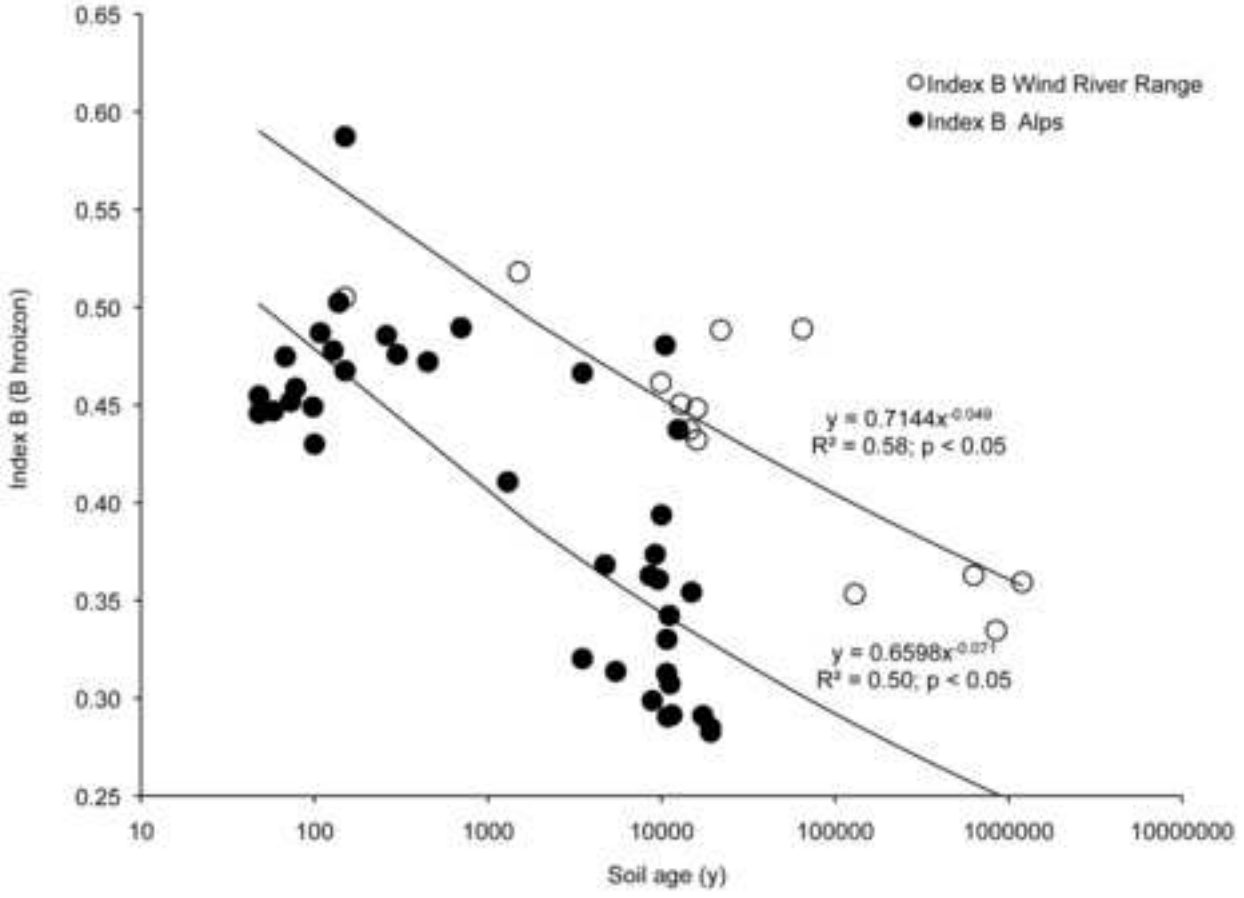

**Figure 6**

Click here to download high resolution image

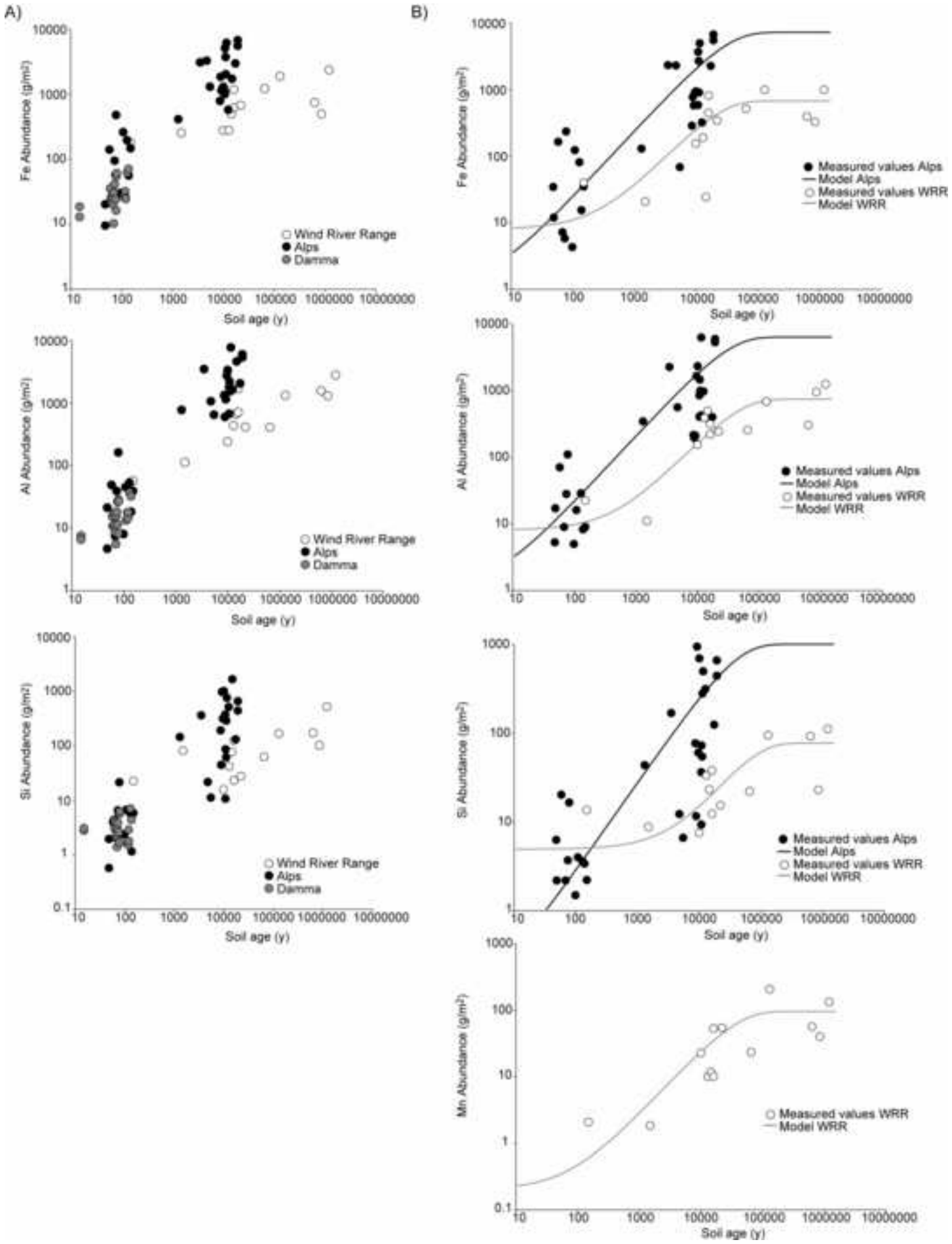

**Figure 7**

**Click here to download high resolution image**